AD-A118 441 FLOW RESEARCH CO KENT WA F/G 20/4
VISUALIZATION STUDY OF TURBULENT SPOTS.(U)
MAY 82 M GAD-EL-HAK, J J RILEY F49620-78-C-0062
UNCLASSIFIED FRC-230 AFOSR-TR-82-0651 NL

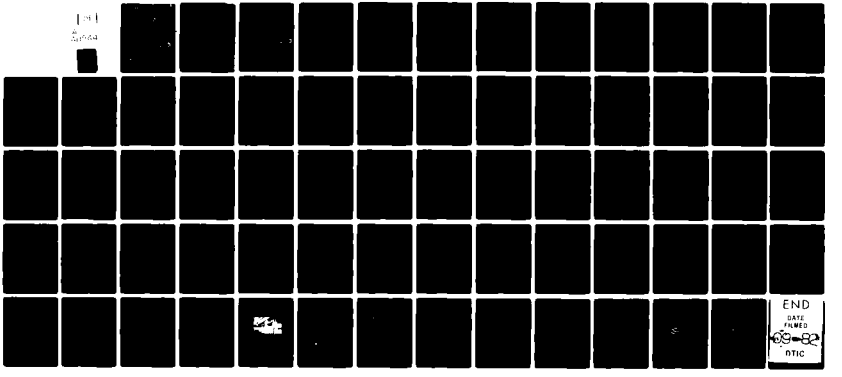

AFOSR-TR- 82-0651

Flow Research Report No. 230

VISUALIZATION STUDY OF TURBULENT SPOTS
(Final Technical Report)

By

Mohamed Gad-el-Hak
and
James J. Riley

Supported under AFOSR Contract F49620-78-C-0082

May 1982

Flow Research Company
A Division of Flow Industries, Inc.
21414-68th Avenue South
Kent, Washington 98031
(206) 872-8500

Unclassified

SECURITY CLASSIFICATION OF THIS PAGE (When Data Entered)

REPORT DOCUMENTATION PAGE	READ INSTRUCTIONS BEFORE COMPLETING FORM
1. REPORT NUMBER AFOSR-TR- 82-0651 / 2. GOVT ACCESSION NO. AD-A118441	3. RECIPIENT'S CATALOG NUMBER
4. TITLE (and Subtitle) Visualization Study of Turbulent Spots	5. TYPE OF REPORT & PERIOD COVERED Final Technical Report 1 May 1980 - 30 April 1982
	6. PERFORMING ORG. REPORT NUMBER FRC Report No. 230
7. AUTHOR(s) Mohamed Gad-el-Hak and James J. Riley	8. CONTRACT OR GRANT NUMBER(s) F49620-78-C-0062
9. PERFORMING ORGANIZATION NAME AND ADDRESS Flow Research Company/Flow Industries, Inc. 21414 - 68th Avenue South Kent, WA 98031	10. PROGRAM ELEMENT PROJECT, TASK AREA & WORK UNIT NUMBERS 61102F 2307/A2
11. CONTROLLING OFFICE NAME AND ADDRESS Air Force Office of Scientific Research Bolling Air Force Base, Building 410 Washington, D.C. 20332	12. REPORT DATE May 1, 1982
	13. NUMBER OF PAGES 64
14. MONITORING AGENCY NAME & ADDRESS(if different from Controlling Office)	15. SECURITY CLASS. (of this report) Unclassified
	15a. DECLASSIFICATION DOWNGRADING SCHEDULE

16. DISTRIBUTION STATEMENT (of this Report)

Approved for public release; distribution unlimited.

17. DISTRIBUTION STATEMENT (of the abstract entered in Block 20, if different from Report)

18. SUPPLEMENTARY NOTES

19. KEY WORDS (Continue on reverse side if necessary and identify by block number)

Turbulent Spots; Laminar Turbulent Transition; Flow Visualization; Entrainment; Growth by Destabilization; Decelerating Laminar Boundary Layers.

20. ABSTRACT (Continue on reverse side if necessary and identify by block number)

An experimental investigation was conducted in the Flow Research 18-m towing tank to study turbulent spots evolving in laminar boundary layers and to modulate the resulting flow fields using salinity stratification, polymer, or unsteady boundary conditions. The research was directed towards understanding the different processes occuring during transition and the

DD FORM 1 JAN 73 1473 EDITION OF 1 NOV 65 IS OBSOLETE S/N 0102-LF-014-6601

Unclassified

SECURITY CLASSIFICATION OF THIS PAGE (When Data Entered)

similarities, if any, between those processes and the intermittent events that characterize the wall region of fully-developed turbulent boundary layers.

A flat plate geometry was used throughout the research program. Flow visualization experiments using fluorescent dyes and laser light were conducted to give global pictures of the different flow fields investigated. Hot-film probe measurements were conducted to give point-by-point data. Two pattern recognition techniques were developed to detect bursts and low-speed streaks in turbulent boundary layers.

Better understanding of the "growth by destabilization" mechanism has been achieved. This mechanism, pointed out in our previous research, governs the lateral growth of all turbulent regions embedded in unstable laminar boundary layers. Striking similarities between the transitional events and the intermittent events in fully-developed turbulent boundary layers have been observed in the present investigation.

Flow Research Report No. 230

Visualization Study of Turbulent Spots*

(Final Technical Report)

By

Mohamed Gad-el-Hak

and

James J. Riley

May 1982

Flow Research Company

A Division of Flow Industries, Inc.

21414-68th Avenue South

Kent, Washington 98031

(206) 872-8500

*Research Sponsored by the Air Force Office of Scientific Research, United States Air Force, under Contract F49620-78-C-0062.

Flow Research Report No. 230
May 1982

Visualization Study of Turbulent Spots*

By

Mohamed Gad-el-Hak
and
James J. Riley

Flow Research Company
Kent, Washington 98031

FOREWORD

Flow Research Company has been contracted by the United States Air Force Office of Scientific Research since 1 May 1978 to study turbulent spots. The first phase of the project was conducted during the period 1 May 1978 - 30 April 1980, and was monitored by Lt. Col. Lowell Ormand. During the Second Phase, 1 May 1980 - 30 April 1982, Captain Michael Francis was the program manager at AFOSR. The National Aeronautics and Space Administration provided partial support for some aspects of the research program, particularly the effects of acceleration/deceleration on the boundary layer.

The research team for this investigation consisted of Drs. Mohamed Gad-el-Hak, Hung Huynh, Thomas McMurray and James J. Riley at Flow Research Company, Professor Ron F. Blackwelder of the University of Southern California, Professor Stephen H. Davis of Northwestern University and Dr. Michael Gaster of the British National Maritime Institute.

*Research Sponsored by the Air Force Office of Scientific Research, United States Air Force, under Contract F49620-78-C-0062.

The list of publications resulting from the present research are as follows:

1. M. Gad-el-Hak, R. F. Blackwelder and J. J. Riley, "Visualization of a Turbulent Spot Using Fluorescent Dye Layers," Bul. Am. Phys. Soc. 24, p. 1142, 1979.
2. M. Gad-el-Hak, R. F. Blackwelder and J. J. Riley, "A Visual Study of the Growth and Entrainment of Turbulent Spots," Proceedings of the IUTAM Symposium on Laminar-Turbulent Transition, p. 297, Springer-Verlag, 1980.
3. M. Gad-el-Hak and J. J. Riley, "Affects of Stratification and Drag Reducing Polymers on Turbulent Spots," Flow Research Note No. 182, 1980.
4. M. Gad-el-Hak and J. J. Riley, "Visualization Study of Turbulent Spots," Flow Research Report No. 162, 1980.
5. M. Gad-el-Hak and J. J. Riley, "The Growth of Turbulent Regions by the Destabilization Mechanism," Bul. Am. Phys. Soc. 25, p. 1091, 1980.
6. M. Gad-el-Hak, J. J. Riley and R. F. Blackwelder, "On the Growth of Turbulent Regions in Laminar Boundary Layers," Journal of Fluid Mechanics 110, p. 73, 1981.
7. M. Gad-el-Hak and S. H. Davis, "A Discussion of Transition to Turbulence in the Decelerating Boundary Layer," Flow Research Note No. 196, 1981.
8. Davis, S. H. and M. Gad-el-Hak, "Transition in Decelerating Boundary Layers," Bul. Am. Phys. Soc. 26, p. 1251, 1981.
9. M. Gaster, "On Transition to Turbulence in Boundary Layers," in Transition and Turbulence, edited by R. E. Meyer, p. 95 Academic Press, 1981.
10. M. Gad-el-Hak and S. H. Davis, "Study of Effects of Acceleration/Deceleration on Turbulence and Transition," Flow Research Report No. 217, 1982.

Copies of No. 2, 6, 9 and 10 are enclosed with this final report.

The following Flow Research films have been produced to summarize the visualization results and have been sent previously to AFOSR:

1. FR Film #40, "Flow Visualization of a Turbulent Spot in a Laminar Boundary Layer."
2. FR Film #41, "Structure of a Turbulent Spot in a Laminar Boundary Layer."
3. FR Film #47, "Effects of Stratification and Drug Reducing Polymers on Turbulent Spots."
4. FR Film #48, "Transition."

The investigation results were presented at seminars at the following institutions: Boeing Company, California Institute of Technology; Cornell University; Massachusetts Institute of Technology; Michigan State University; NASA-Ames; NASA-Langley; National Academy of Sciences; Naval Postgraduate School, Naval Ship R&D Center; Ohio State University; Stanford University; University of Colorado; University of Notre Dame; University of Southern California; University of Stuttgart; University of Washington; University of Wisconsin-Madison; and Washington State University.

We would like to acknowledge the valuable help of our colleagues at Flow, especially H. Huynh, T. McMurray and R. Srnsky. Captain M. Francis of AFOSR continuous support is greatly appreciated.

Table of Contents

1. Introduction

A research investigation aimed at improving our understanding of turbulence and transition was conducted at Flow Research Company. Experiments were conducted in the 18-m towing tank using a flat plate. Artificially generated turbulent spots were allowed to grow in a laminar boundary layer. To illuminate the nature of their growth within the unstable laminar boundary layer, the spots were modulated using salinity stratification, polymers, or unsteady boundary conditions. Transition was also triggered by decelerating the flat plate. Turbulent boundary layers were generated by tripping, and particular attention was given to the organized structures in the wall region and to comparisons of these structures with those associated with the growth and destabilization mechanisms found in transitional flows.

The process of transition on a flat plate at zero angle of attack has been subjected to numerous intensive investigations. It was first studied by Burgers (1924), Van der Hegge Zijnen (1924), and in greater detail by Dryden (1934, 1936, 1939). Near the leading edge, the boundary layer is always laminar, provided there is no separation, and it becomes turbulent further downstream. Early theoretical work of Tollmien (1931) and Schlichting (1933) considered the initial growth of infinitesimal, two-dimensional disturbances superimposed on the laminar flow. When the Reynolds number exceeded a critical value, they found that the initial disturbance grew exponentially with time. The theoretically predicted growth rate was confirmed experimentally by Schaubauer & Skramstad (1948). Provided that all sources of external disturbance are sufficiently small, they showed that transition is preceded by the appearance of weak oscillations as predicted by the linearized theory of laminar instability. Those oscillations were initially in the form of two-dimensional instability waves with a wave speed about one-third of the free-stream velocity and a wave-length several times the boundary-layer thickness. Klebanoff, Tidstrom & Sargent (1972) found that these waves rapidly developed three-dimensional aberrations culminating in a larger growth rate and the appearance of a velocity 'spike' before the flow broke down into turbulence.

Kovasznay, Komoda & Vasudeva (1962) mapped the region of concentrated vorticity in a boundary layer prior to breakdown. The total length of the region in which the vorticity exceeds the value obtained in a Blasius boundary layer was found to be approximately four times the boundary-layer thickness.

Their results were consistent with the visualization study of Hama, Long & Hagarety (1957), which suggests that the amplification of small disturbances becomes associated at some stage with the concentration of vorticity along discrete lines, which subsequently distort into vortex loops within the boundary layer. The vortex loops themselves go through a process of distortion and extension, finally resulting in the breakdown into turbulence.

Since the three-dimensionality seems an important aspect of the growth of small disturbances, Gaster & Grant (1975) studied experimentally the formation and development of a wave packet generated in a laminar boundary layer on a flat plate. The packet was artificially generated by a short-duration acoustic pulse, which was injected through a minute hole on the plate. Their experimental results were compared with a linear model of a wave packet proposed by Gaster (1975). The comparison was quite good close to the source, but was not maintained far downstream, where the experimental packet showed various irregularities. The wave-crests of the propagating wave packet became distorted when the amplitude of the initial disturbance was large enough. These distortions of the wave fronts were associated with steep shear layers within the boundary layer, and with high-frequency bursts of oscillation that eventually led to embryo turbulent spots (Gaster 1978).

The appearance of turbulent spots within a laminar boundary layer had been first reported by Emmons (1951) who observed spots which were created randomly as the boundary layer underwent transition. On the basis of visual observation in a water table, Emmons concluded that randomly generated spots grow uniformly and act independently of one another as they are swept downstream by the flow. He developed a model which related some statistical properties of the spots to a single source-rate density function. Elder (1960) used dye to visualize the turbulent spots. He observed a point-like breakdown, in which the spots originate from a very small volume within the boundary layer. He investigated the conditions required for breakdown to turbulence, and the degree of interaction between adjacent spots. Elder concluded that breakdown is determined by local conditions, and is essentially independent of the Reynolds number and boundary-layer thickness. A critical Reynolds number is only required in order to amplify small disturbances, whereas sufficiently strong disturbances may burst into turbulence almost instantaneously regardless of the Reynolds number. Elder observed the interaction between two

artificially generated spots which were displaced laterally, and concluded that there was no noticeable alternation in the growth rate of one spot owing to the presence of the other. Thus, he verified a major assumption in Emmons' model for the statistical properties of the spots.

Schubauer & Klebanoff (1956) continually initiated turbulent spots in a laminar boundary layer and measured the velocity signals and celerities associated with the spot. They also reported a 'calmed region' immediately following the spot which was more stable than the surrounding flow.

Coles & Barker (1975) used conditional sampling techniques to study the spot's velocity field. By assuming a two-dimensional mean flow, they educed the streamline pattern in the center of the spot and suggested that the spot grows not only by entraining irrotational fluid from the ambient free stream, but also by entraining fluid from the ambient laminar boundary layer.

Wygnanski, Sokolov & Friedman (1976) also used conditional sampling methods to obtain the average shape of a spot and the mean flow field in its vicinity. They found that fluid deep in the laminar boundary layer overtakes the rear interface of the spot, and is entrained into it. Fluid outside the boundary layer passes over the ridge of the spot and is entrained through the leading interface. Zilberman, Wygnanski & Kaplan (1977) extended the Wygnanski et al. work to track the structure of the turbulent spot as it merges and interacts with a turbulent boundary layer generated by a row of spherical trips. They showed that the spot structure tracked in the turbulent boundary layer retains its identity and suffers a negligible loss of intensity. The structure exhibits features in detailed agreement with those of the outer region of the turbulent boundary layer, such as a convection speed of $0.9U_\infty$, and is consistent with existing two- and three-point space-time correlations.

Cantwell, Coles & Dimotakis (1978) conducted laser-Doppler velocity measurements for the flow in the plane of symmetry of a turbulent spot. Their measurements suggest that strong entrainment occurs along the outer part of the rear interface and also in front of the spot near the wall, while the outer part of the forward interface is passive. The experimental investigation of Wygnanski, Haritonidis & Kaplan (1979) in the region trailing the turbulent spot in a laminar boundary layer revealed the existence of a pair of oblique Tollmien-Schlichting wave packets. The breakdown of this ordered motion into a new turbulent spot was accompanied by the appearance of an intense shear layer inclined to the wall.

More recently, Van Atta & Helland (1980) conducted exploratory measurements of temperature fluctuations to study the structure of turbulent spots generated on a fully heated flat plate. They addressed a number of questions that have been raised by previous investigators regarding the mechanism by which a turbulent spot mixes the fluid in the boundary layer to transfer momentum and scalar properties during transition.

An important aspect of the turbulent spot, and indeed all such regions of localized turbulence, is the process by which the spot grows, incorporating previously non-turbulent fluid. In particular, near the plate the exterior fluid is rotational, and the lateral growth mechanism there might be different from classical entrainment. Charters (1943) was the first to note that the transverse growth rate of a turbulent region embedded in an unstable laminar boundary layer is significantly larger than usual turbulent entrainment rates. He called this process 'transverse contamination' and noted that it was independent of the originating cause. Corrsin & Kistler (1955) suggested that the spreading of a turbulent shear region into a shearing laminar region might be governed by a different propagation mechanism than that governing the spreading of turbulence into an irrotational fluid. They speculated that a destabilization of the already rotational flow could occur in addition to a transmission of random vorticity be direct viscous action (entrainment). Morkovin (1969) noted that the transverse contamination process discovered by Charters (1943) has been the subject of only one further study, by Schubauer & Klebanoff (1956), who examined the turbulent wedge behind a roughness element placed in a laminar boundary layer.

An alternative vehicle for the study of the transition process is the decelerating-plate experiment. Here a plate of length L moves steadily normal to its leading edge. L is short enough that the Blasius layer remains laminar along its full length. At time $t = 0$, the plate is decelerated rapidly to a new constant final speed. Flow visualization seemingly shows that a sequence of two-dimensional structures, three-dimensional structures, hairpin vortices and then turbulent bursts results. As the deceleration takes place, the instantaneous velocity profiles become inflectional. If the inviscid instability associated with the instantaneous inflection point has large enough growth rate, then there is an instability which will cause two-dimensional waves to grow in the unsteady flow (Drazin & Reid, 1981).

Subsequently, there is a breakdown (perhaps a new instability of the two-dimensional structure) into three-dimensions, an intensification of the three-dimensional structure, the development of hairpin vortices and then turbulent bursts.

The deceleration experiment differs from the fixed-plate experiment in several respects. First, given the inflectional character of the initial instability, the two-dimensional waves are expected to have substantially larger growth rates than their Tollmien-Schlichting counterparts (Drazin & Reid, 1981). Hence, there may be developed a "clean," strongly two-dimensional wave field during the initial stages of the transition process. This contrasts with the mixed two- to three-dimensional field for the fixed plate experiment (Anders & Blackwelder, 1979). Careful point measurements are required to determine whether this is the case. If this is the case, it suggests the study of this instability in order to determine the mechanism and characteristics of the development of three-dimensionality. The isolation of this problem is one of the main advantages of the deceleration experiment over the fixed-plate experiment. If the above picture is correct and there is a well-defined transition from laminar two-dimensional waves to laminar three-dimensional waves through an instability process, one has identified a major link in the transition process. An understanding of this instability would allow one to contemplate means of interferring with the process to delay transition or reinforcing the process to foster transition. It would give one a handle in examining the subsequent evolution to hairpin vortices since these might be examined through the nonlinear evolution of the three-dimensional structure. In summary, the deceleration experiment might be one that clearly separates two-dimensional from three-dimensional structures and allow analysis of the change from one to the other.

In the present investigation we addressed some of the questions raised above. Experimental and numerical investigations were carried out to determine the mechanics of transition on a decelerating flat plate. We also investigated the effects of acceleration and deceleration on the growth rates of turbulent spots generated by disturbing a laminar boundary layer at a point.

The preliminary results we have so far point to impressive similarities between transitional events and the so-called bursting cycle in a turbulent boundary layer. If the events prove to be very similar, then one can apply

knowledge gained in a transitional flow field to an equivalent turbulent flow field. Numerical and theoretical work in the transition problem is probably more tractable, and this sets the stage for understanding the more complicated turbulence problem.

2. Experimental Approach

2.1 Towing Tank System

The flat plate used in the present experiment was towed at a speed up to 100 cm/sec through a towing tank that is 18 m long, 1.2 m wide, and 0.9 m deep. Figure 1 is a photograph of the towing tank. The flat plate was rigidly mounted under a carriage that rides on two tracks mounted on top of the towing tank. During towing, the carriage was supported by an oil film which insured a vibrationless tow, having an equivalent free-stream turbulence of about 0.1 percent. The carriage was towed with two cables driven through a reduction gear by a 1.5 hp Boston Ratiotrol motor. The towing speed was regulated within an accuracy of 0.1 percent. The main frame supporting the tank could be tilted and levelled by adjusting four screw jacks. This feature was essential for smooth operation of the carriage, whose tracks are supported by the main frame. The towing tank was designed so that flow visualizations can be made from the top, sides, bottom and ends, the bottom and side walls are made of 19 mm thick plate glass with optical quality. The end walls are made of 38 mm thick Plexiglas.

2.2 Model and Test Conditions

Three different flat plates were built at different stages of the investigation. During the early phases of this investigation, our first flat plate was made of Plexiglas. To improve the experimental configuration, a second plate was constructed in a modular form. It was made of NOMEX honeycomb covered on the bottom side with fiberglass resin and on the top side with the working Plexiglas surface. The latest version, sketched in Figure 2, utilized an aluminum frame to provide a flat bed for the Plexiglas working surface. We believe that this arrangement insures a flat surface to within 0.2 mm that will not change with aging. The gaps in the aluminum frame are filled with light-weight styrofoam and the frame is painted with marine enamel to prevent corrosion. The whole structure is buoyant in water, and is easy to adjust to prevent the middle of the plate from sagging under its own weight.

The working surface is smooth and is 210 cm long and 106 cm wide. Care is taken to avoid leading-edge separation and premature transition by having an elliptic leading edge and an adjustable lifting flap at the trailing edge.

The flap was adjusted so that the stagnation line near the leading edge was located nearer the working surface.

In the range of towing speeds 0 to 80 cm/sec, a laminar boundary layer is generated on the working surface. Trips are used to generate a fully developed turbulent boundary layer, and a single trip is used to generate a single turbulent wedge embedded in the laminar boundary layer. The roughness elements (trips) are brass cylinders with 0.32 cm diameter and 0.25 cm height, placed 30 cm behind the leading edge with their axes perpendicular to the flat plate. To generate turbulent spots, any of three 0.4 mm diameter injection holes located at different locations on the working surface provide a small squirt of water into the laminar flow. The injection is controlled with a constant-head tank and a solenoid valve.

The Reynolds number based upon a towing speed of 40 cm/sec and upon the displacement thickness at the first injection hole was 740, well above the critical Reynolds number for linear instability. When not disturbed, the boundary layer on the working surface remained laminar until tripped close to the trailing edge. The plate was positioned 5 cm from the tank walls and the circulation around the plate generated by the flap was such that disturbances were not communicated from the bottom surface to the top (working) surface.

2.3 Flow Visualization

The turbulent regions were made visible by novel techniques which utilized fluorescent dye, i.e. dye which is visible only when excited by a strong light source of the appropriate wavelength. This provided an extra degree of freedom in observing the flow because both the dye and light location could be controlled within the limitations of the experimental apparatus. A 5 watt argon laser (Spectra Physics, Model 164) was used with a cylindrical lens to produce a sheet of light that could be projected perpendicular to each of the three axes as required. The light sheets were approximately 1 mm thick, which was sufficient to resolve the large structure within the turbulent regions. Recently, we have started experimenting with mirrors mounted on an optical scanner having a 720 Hz natural frequency (General Scanning, Inc.) driven by a sine-wave signal generator of the desired frequency to generate a sheet of laser light. The results so far are very encouraging since the sheet generated is 'cleaner' as compared to the one generated by the cylindrical lens, and can be made

smaller, if desired, by the use of spherical lenses. The frequency of the sine-wave is usually set equal to the shutter speed of the camera.

Three different methods of dye injection were employed. In the first, a dye sheet seeped into the laminar boundary layer through either of two spanwise slots. The first is 0.15 mm wide, 30 cm long and is located 35 cm downstream of the leading edge. The second slot is 0.15 mm wide, 50 cm long and is located 75 cm downstream of the leading edge. Each slot was milled at a 45° angle inclined towards the trailing edge to minimize the flow disturbance. Each slot was divided into four separate sections, each with its own dye source, so the spanwise mixing and diffusion of turbulent fluid could be studied. The dye remained on the plate surface until the turbulent spot caused it to lift and diffuse.

Discrete lines of dye could be allowed to seep into the laminar boundary layer by masking the spanwise slot with 32 cm long strip of electrical tape, in which thirty longitudinal slots, 1 cm apart and 0.5 cm long, were cut with a surgical knife. The resulting dye lines were less than 0.5 mm wide near the trailing edge of the plate. A new dye injection system has been added to the working surface to inject different color streaks of dye. Two rows of minute holes (0.4 mm diameter) in the working surface are supplied with dyes from two separate wells under the plate. The first row contains 28 holes, separated center-to-center by 1 cm, and is located 64 cm downstream of the nose. The second row contains 27 holes, each shifted by 0.5 cm in the spanwise direction relative to a corresponding hole in the first row, and is located at $x = 65$ cm. The alternating color dye lines seeping from the holes stay next to the surface until lifted by an upward motion. Better visualization of three-dimensional motion was obtained because the motion of the dye lines in the spanwise direction was clearly visible whereas uniform dye sheets obscured this motion.

Dye was also placed in the flow field by laying several thin, horizontal sheets prior to towing the plate. These layers remained thin, about 1 mm in thickness, due to the inhibition of vertical motion caused by introducing a weak saline stratification in the tank. Fluorescein, Rhodamine-B, and Rhodamine-6G dyes were used which fluoresced green, dark red and yellow, respectively, when excited by the argon laser. In a floodlight, the first two dyes fluoresced green and dark red, while Rhodamine-6G had a faint red color. The alternating sheets of different colors remained quiescent until disturbed

by the turbulent spot on the towed plate. The motion of the potential flow could also be observed since dye layers existed in the potential region also.

The visualization information was obtained using 35 mm photographs and 16 mm ciné films. The cameras were typically controlled by microswitches which filmed the spot at predetermined times after its generation. The 16 mm films were analysed by a stop-action projector.

We have started experimenting with 10-20 micron titanium dioxide coated mica particles, manufactured by the Mearl Corporation, for flow visualization.* These disk-shaped platelets (thickness << diameter) align themselves along the axis of principal normal stress in the flow field, so that they reveal more or less instantaneous patterns of the flow. This technique will complement the dye visualization techniques that show integrated diffusion effects, and is suited for visualizing coherent structures in turbulent and transitioning flows, and whenever wave patterns are present.

2.4 Stratification and Polymer Additives

A stratified fluid of a predetermined density profile could be made by feeding salt water, layer by layer with increasing density, into the tank through two channels along the tank bottom. The salinity of the water and its feeding rate determined the density profile in the undisturbed tank. A linear density profile is characterized by its Brunt-Väisälä frequency N, defined as

$$N \equiv \frac{1}{2\pi} \left(\frac{-g}{\rho_0} \frac{d\rho}{dy} \right)^{1/2} ,$$

where g is the gravitation acceleration, ρ_0 is a reference density (1 g/cm^3), and $\rho(y)$ is the undisturbed density profile.

The Brunt-Väisälä frequency provides a convenient measure of the time scale at which stratification effects are important. It is the natural frequency of oscillation of a fluid particle under infinitesimal perturbation. In the present experiment, N varied in the range 0-0.7 Hz.

The polymer used in the present experiment was Polyox, WSR-301 (polyethylene oxide) manufactured in powder form by Union Carbide Corporation. It

---

*Our thanks to Professor S. Widnall of MIT for supplying us with valuable information regarding these particles.

has a molecular weight of about 4×10^6, and was used in concentration of 50 parts per million (p.p.m.) by weight. A uniform dispersion of the Polyox resin in the towing tank water was necessary for good dissolution. If the resin powder was not properly dispersed, the partially dissolved, wetted particles agglomerated and formed gels which would dissolve only with prolonged high-speed agitation. However, such prolonged high-speed agitation must be avoided to prevent shear degradation of the resin. A novel method was used in the present study to dissolve the polymer in the water. An aspirator driven by 80-psi compressed air was used to lift the dry polymer powder from its container into a 25 mm PVC pipe. The pipe released the mixture of air and polymer near the bottom of the towing tank. The air provided an ideal medium for dispersing the resin. The polymer mixed well with the water without forming gels, and the air escaped to the surface.

2.5 Hot-Film Probes

Subminiature boundary-layer hot-film probes (TSI Model 1260) were used in the present investigation to measure the longitudinal mean and fluctuating velocities. Each probe diameter is 0.025 mm and its sensing length is 0.25 mm. The probe support is 0.9 mm diameter and 32 mm long. A probe traverse powered by a stepping motor and controlled through an APPLE II minicomputer was used for surveying the laminar, transitional, and turbulent boundary layers. For data acquisition and analysis, a NOVA 800 and PRIME 750 minicomputers were used.

2.6 Pattern Recognition Techniques

To better understand the intermittent events occurring in the wall region of a turbulent boundary layer, two pattern recognition programs have been developed for the present investigation. The instantaneous longitudinal velocity from one or more hot-film probes placed near the wall is processed digitally searching for recognizable patterns or structures. The first program is a low-speed streak detection scheme. The streamwise velocity signals from three hot-film probes are compared by the algorithm. The probes are located 10 wall units (ν/u^*) above the plate at the same streamwise position with a spanwise separation of approximately 20 wall units. Thus the total array spanned 40 wall units which is approximately half the average low-speed streak spacing.

A low-speed region is identified by the algorithm when all three signals are less than the local mean velocity by some predetermined threshold value and the middle signal is less than the velocity on either side. This technique allows a direct comparison with the visualized streaks in the buffer layer and also yields quantitative data such as histograms of streak lengths.

The results of the algorithm were compared with iso-velocity contours obtained from a rake having a wider spanwise extent. The comparison showed that the detection picked out the streaks exceedingly well and secondly that the streaks meander in the spanwise direction so that often a single streak crosses the probes two or more times resulting in multiple detections.

The second pattern recognition algorithm is a burst detection scheme using the variable-interval time-averaging (VITA) technique developed by Blackwelder & Kaplan (1976). A single hot-film probe located at 20 wall units above the wall is used for burst detection. The program counts the number of bursts that occur near the wall as well as their intensities. A listing in FORTRAN of both algorithms is given in Appendix II and III. Appendix I is a listing of the conventional statistics program (mean and root-mean-square) needed for both pattern recognition algorithms.

3. Results and Discussion

3.1 Turbulent Spots

Several reference runs were made to check the overall quality of the towing system and the established flow field. Conventional food-coloring dye was allowed to seep from the spanwise slot and several holes near the leading edge. Dye seeping from the leading-edge holes indicated that the stagnation point was slightly toward the working side of the plate and no separation occurred. When unperturbed, the dye from the slot remained on the surface and had a glassy smooth appearance over the entire length of the plate, indicating that a laminar boundary layer was maintained until the end of the plate, where the Reynolds number was $U_\infty x/\nu = 1.3 \times 10^6$ for a towing speed $U_\infty = 60$ cm/sec. When disturbed by the solenoid injection of fluid through the hole at $x = 33$ cm, a spot having the classical arrowhead shape could readily be observed as the turbulence removed the dye from the wall layer. The developing shape of several spots was mapped to determine the virtual origin. It occurred at $x = 43 \pm 2$ cm, i.e. 10 cm downstream of the ejection hole, and at $t = 0.63 \pm 0.1$ sec after the ejection.

The extra degree of freedom provided by using fluorescent dye was found to be quite effective in revealing the structure of a turbulent spot. To elucidate the manner in which the spot (or any turbulent region in an unstable laminar boundary layer) spreads laterally, a turbulent wedge, generated by introducing a roughness element into the unstable laminar boundary layer, was investigated both visually and with probe measurements. The visualization results were reported in detail in our Journal of Fluid Mechanics' Paper (Vol. 110, p. 73, 1981) and the reader is referred to it for further information. Here we reiterate the important highlights.

It was found that the spot grew normal to the plate by classical turbulent entrainment, in much the same way that a turbulent boundary layer grows. However, the growth in the spanwise direction, which has a rate of roughly an order of magnitude larger than the growth rate normal to the plate, was not due to classical entrainment. Our results strongly suggest that the spanwise growth may be due to a destabilization process, as suggested by Corrsin & Kistler (1955). We term this process 'growth by destabilization,' which manifests itself as follows: the turbulent eddies within the spot appear to

induce perturbations into the surrounding unstable laminar boundary layer which rapidly grow and break down, forming new turbulence, without ever being in direct contact with the older turbulence.

No dominant vortex was observed in the visualizations, but instead the spot appeared to be composed of a collection of somewhat independent, random eddies, much as in a turbulent boundary layer.

A qualitative picture of the different dynamic regions of a spot is given in Figure 3. It shows a schematic of an x-y cut through a sector of the spot (excluding the region near the wingtips). Region I, the head of the spot, is a result of turbulent fluid being swept over the laminar boundary layer. This region, being cut off from the turbulence near the plate and its associated generation processes (e.g. bursting), appeared fairly passive, in agreement with the measurements of Cantwell et al. (1978).

However, Region I exhibits a pronounced overhang over Region II, the laminar boundary layer below and ahead of the spot. In Region II, perturbations due to the presence of the spot are felt upstream of the spot, but the breakdown to turbulence does not occur until the spot rides over this laminar region. To determine whether the perturbation and growth of the instability ahead of the spot are important, or whether the flow is driven unstable by the overhang region, a visualization experiment was conducted using two alternating horizontal sheets of light. The first was at the wall, and the second was at a laminar boundary layer thickness above the wall. The two elevations could be alternatively seen at a rate of approximately 48 cycles/sec. The high oscillation rate allowed the two planes to be viewed almost simultaneously; i.e. with time separations that were small compared to the time scales of the turbulent spot. The resulting film (Flow Research Film No. 48) revealed that the turbulent region at $y = \delta$ extended far upstream of the simultaneous turbulence at the wall. This phenomena, called an overhang, had been documented before along the centerline of the spot using hot-wire anemometers. However, the film showed the same phenomenon occurred everywhere along the leading edges of the spot and it appeared everywhere simultaneously; i.e. it was not occurring at random or in an oscillating mode. Furthermore, the oscillations at the wall only occurred whenever there was an overhang at $y = \delta$ suggesting that the outer turbulence does indeed trigger the oscillating motion at the wall.

The localized transition to turbulence was also briefly explored by using a brine dye laid on the plate before towing began. The dye was heavier than the surrounding fluid and was only removed slowly by the laminar flow. However, when a spot passed by, the vigorous turbulent action rapidly mixed the dye with the surrounding fluid. Thus the brine dye provided a convenient means of observing the laminar-turbulent transition process on the plate. As the turbulent spot drew near, definite imprints within the laminar could be observed. Presumably this was imposed from the overhang structure in agreement with the previous results. The dye on the surface allowed the observation of certain features prior to and during the passage of the spot. In particular, the following sequence of events was observed. As the spot approached, weak motions were observed until, quite suddenly, a pocket would form similar to those observed by Falco (1978). As the disturbance associated with the pocket was advected downstream, a track or signature of the disturbance was left along the surface. The front edge of the spot was marked by a series of occurrences of such pockets. As the spot passed over the portion of the plate under observation, similar events would occur intermittantly over the entire surface, generating pockets and subsequent tracks. After the spot had passed, these tracks appeared to be the streaky structure previously observed in the wake of the spot (see the discussion of Region V below).

Falco (1978) has suggested that the pockets are possibly associated with a bursting-like event involving the lift-off of a horseshoe vortex. If that is the case, then the track quite possibly consisted of the counter-rotating vortices of the horseshoe vortex, and hence would be similar to the counter-rotating vortices so often associated with the low-speed streaks in a turbulent boundary layer (see, e.g., Blackwelder and Eckelmann, 1979).

The front of the spot appears to be growing mostly in Region II, as the laminar boundary layer breaks down. New turbulence is thus added to the lower front part of the spot, which is again consistent with the measurements of Cantwell et al. (1978).

Region III appears to be dynamically very similar to a classic boundary layer over a flat plate. The growth rates normal to the plate are about the same for the turbulence in Region III and for a turbulent boundary layer. Furthermore the entrainment of nonturbulent fluid in planes normal to the wall appeared to involve large-scale eddies in a gulping process similar to a fully developed turbulent boundary layer.

As the streamwise mean shear acts upon the spot, it exposes a region of fluid, Region IV, which was originally in the lower part of a turbulent-boundary-layer-like flow, but which is now left to interact with the oncoming laminar boundary layer and the external potential flow. This turbulent fluid is still rather active, and quickly begins entraining the fluid above it. This produces the growth of the spot in the rear as observed in x, z planes.

Finally, Region V denotes the 'calmed' region following the spot. The streaks of dye aligned with the streamwise direction seem to be the dominant characteristics in the visualization results shown here and by others. It is commonly believed that these streaks are the result of streamwise vortices lying near the wall which raise the dye seeping into the calmed region of the spot.* However, this region remains laminar, possibly due to the stable velocity profile in the region.

Cross-sections of the spot off the center-line are similar to that sketched in Figure 3, except the relative lengths of the different regions will vary in the spanwise direction. In the region near the wingtips, the ciné films show that the flow approaching the wingtips becomes highly contorted and breaks down as it passes into the vicinity of the wingtips in a manner similar to that seen at other locations around the spot.

The detailed mechanism of how the turbulence induces fluctuations into the unstable boundary layer is not known. However, the visualization results lead to a reasonable qualitative picture of how the breakdown occurs. The turbulence in the spot induces pressure fluctuations in the unstable boundary layer exterior to the spot. Previous measurements have shown that the effects of these pressure fluctuations are felt many laminar boundary layer thicknesses upstream of the spot (see, e.g., Wygnanski et al., 1976; and Cantwell et al., 1978). Because the boundary layer is unstable, these fluctuations are expected to grow. As the spot approaches a particular fluid element, the pressure fluctuations become very large, especially in Region II below the overhang. The laminar flow finally breaks down into turbulence, and hence becomes part of the spot. However, it is not clear whether this breakdown is due to a gradual growth of the induced disturbances (and hence linear stability theory is

*It is likely that these streaks are just the remnants of the sublayer streaks in Regions III and IV.

relevant in describing the process), or whether the breakdown is catastrophic and highly nonlinear.

Since the laminar boundary layer is unstable to Tollmien-Schlichting waves, it is tempting to suggest that the induced disturbances will grow accordingly. This does not seem to be the case, however. The wavelengths observed using the discrete dye lines technique are about 1-2 laminar-boundary-layer thicknesses; too small for Tollmien-Schlichting waves. In addition, the growth rates of the disturbances are too large when compared with the linear theory. However, since the laminar boundary layer near the spot is distorted from the Blasius profile, a more detailed calculation and comparison is required before the linear Tollmien-Schlichting mechanism can be eliminated.

Whenever sinuous motion occurred in the dye lines upstream of the spot, usually only 1-2 wavelengths were visible. However, since a large amplitude is needed before they can be seen, it is possible that these oscillations were part of a longer wave-train. The spanwise extent of the oscillations was nominally one wavelength. As indicated earlier, the growth rate of the oscillations prior to breakdown was quite large. This evidence has led to the speculation that the observed oscillations may be similar to those observed by Klebanoff et al. (1962) following the nonlinear growth of Tollmien-Schlichting waves just prior to breakdown in an unstable laminar boundary layer. That is, the oscillations associated with the 'spike' had a wavelength of roughly one boundary-layer thickness, were of limited spanwise extent and exhibited only a few oscillations before breaking down into complete chaos, i.e., turbulence. Because Klebanoff et al. had a more controlled experiment, their observed oscillations and breakdown were more repeatable than in the present experiment. That notwithstanding, the similarities between the two is highly suggestive that similar mechanisms may be responsible for the observed breakdown in both experiments. In Section 3.4, we will explore this point furher.

The evidence suggests that the spanwise growth is governed by the disturbance field of the turbulent eddies in the vanguard of the spot and the stability characteristics in the surrounding laminar boundary layer. As a turbulent eddy grows to elevations outside the laminar boundary layer, it is carried downstream over the unstable laminar regions by the free stream. The velocity field of the eddy induces disturbances into the unstable laminar boundary layer which propagate and grow according to the dominant instability mechanism

and ultimately break down into turbulence. Thus the leading edge of the spot is not a convected interface, but is a locus of points where the fluctuations have broken down into turbulence.

This hypothesis is consistent with the results from the dilute polymer solution experiments. Since less dye seemed to have been removed from the plate under these conditions, the polymers seemed to have suppressed the turbulence intensity. Also the lateral growth rate was reduced by about 15 percent, resulting in a more elongated spot. The experiments confirm that the polymer effects are closely associated with wall phenomena. For while the addition of polymer seems to modulate the growth by destabilization mechanisms, it does not seem to affect the entrainment mechanism.

Stratification was also used to modulate the turbulent spot. The stratification inhibited the vertical growth of the turbulent spot. The effect is more pronounced as the density gradient, and hence the Brunt-Väisälä frequency, is increased. The head of the spot collapsed after about 1/4 Brunt-Väisälä period, much the same as a wake collapse in a stratified fluid. There did not seem to be any effect on the spanwise growth as measured by the spreading angle of the spot.

The final picture which emerges from this set of experiments is that the growth of turbulent spots in the spanwise direction is an order of magnitude greater than the growth normal to the plate, and that the spanwise growth is by destabilization of the surrounding unstable laminar boundary layer. Although a conceptual model is suggested which correlates the present observations, further work is required to understand fully this new growth mechanism.

3.2 Accelerating/Decelerating Flows*

3.2.1 Theoretical Considerations

When a Blasius boundary layer is subjected to deceleration, two-dimensional vorticity waves are observed. These waves do not stay two-dimensional for very long, and three-dimensional effects become pronounced. If one wishes to study the instability of the finite amplitude two-dimensional wave system to three-dimensional instabilities, one may proceed along the following lines.

---

*The work described in this section was cosponsored by AFOSR and NASA-Ames. Much of the material in this section appeared in Flow Research Report No. 217.

i. Basic State

The flow that initially becomes unstable is an unsteady boundary layer caused by plate deceleration. The initial and final states are Blasius layers. Hence, one should solve (Rosenhead, 1963, and Schlichting, 1968):

$$\bar{\psi}_{yt} + \bar{\psi}_y\bar{\psi}_{xy} - \bar{\psi}_x\bar{\psi}_{yy} = \bar{\psi}_{yyy} \tag{1a}$$

$$\bar{\psi}(x,\infty,t) = 0 \qquad , 0 < x < L \ , \ t \geq 0 \tag{1b}$$

$$\bar{\psi}_x(x,0,t) = 0 \qquad , 0 < x < L \ , \ t \geq 0 \tag{1c}$$

$$\bar{\psi}_y(x,0,t) = -U_w(t) \qquad , 0 < x < L \ , \ t \geq 0 \tag{1d}$$

$$\bar{\psi}(x,y,0) = \bar{\psi}_B(x,y) \qquad , 0 < x < L \ , \ t < 0 \ , \ y \geq 0 \tag{1e}$$

Equation (1a) is the nondimensionalized longitudinal momentum equation, with the familiar boundary layer approximations applied. Here, $U_w(t)$ is the speed history of the plate, $\bar{\psi}_B$ signifies the stream-function of the Blasius solution prior to deceleration and $\bar{\psi}$ denotes the stream-function for the two-dimensional, unsteady boundary layer.

The resulting unsteady boundary layer

$$\bar{\psi} = \bar{\psi}(x,y,t) \tag{2}$$

is a combined Blasius-Rayleigh solution (Stewartson, 1951).

ii. Linear Stability Theory

The onset of shear instabilities is obtained by linear stability theory of solution (2). $\bar{\psi}$ is unsteady, but one could argue (Davis, 1976) that it is sufficient to examine the 'quasi-steady' stability problem in which the instantaneous profiles

$$\bar{\psi}_s = \bar{\psi}_s(x,y;t_o) \equiv \bar{\psi}(x,y,t = t_o) \tag{3}$$

are treated as steady, parallel flows and an Orr-Sommerfeld system is examined. Such an approximation is valid if the time rate of change of $\bar{\psi}$ (measured by a viscous diffusion time) is slow compared to the rate of growth of disturbances of $\bar{\psi}_s$ (measured by a convection time). This is guaranteed if the steady-flow

Reynolds number is sufficiently large. The solution of this Orr-Sommerfeld equation yields a critical $R_{\delta*}$ for each profile (parameterized by t_o).

Thus, there is a 'most dangerous' profile; this corresponds to $t_o = t_{o_c}$. t_{o_c} is a measure of the time delay between deceleration and the appearance of the first two-dimensional instability. Presumably, the instability is due to the inflectional nature of the profile. Here the point of inflection at $t = 0$ is at the wall and moves outward on a diffusion time scale. If the point of inflection is too close to the wall, viscous effects stabilize the profile. If on the other hand it is too far from the wall, the inflection point is in a region where $\overline{U}$ is very small so the instability is not important. The 'most dangerous' profile corresponds to an intermediate value of t_o.

3.2.2 Flow Visualization Results

Visualization experiments were conducted to determine the effects of acceleration and deceleration on the growth rate of turbulent spots. Plan views of spots generated by distrubing an unstable laminar boundary layer were analyzed using a digitizer connected to an APPLE-II microcomputer. The initial towing speed varied in the range 20 to 60 cm/sec, yielding a momentum thickness Reynolds number at the injection hole 400 to 900. The flat plate was then either accelerated or decelerated to a terminal speed at a rate that varied in the range 1 to 60 cm/sec^2.

Spots growing on the flat plate towed at uniform speeds subtended a half-angle of $10 \pm 0.5°$, consistent with previous data (Gad-el-Hak et al., 1980; 1981). Spots growing on an accelerating plate subtended a half-angle slightly smaller. For the maximum acceleration rate in the present experiment, the plate accelerated from 40 cm/sec to 60 cm/sec in one second ($\partial U/\partial t \sim 20$ cm/sec^2), and the half-angle was 9°. The reduction in the spanwise growth observed in the present experiment is then not very significant. The accelerating boundary layer is expected to be more stable than the Blasius boundary layer, analogous to a boundary layer with favorable pressure gradient. Wygnanski (1980) reported a spanwise angle of the spot of less than 5° in the presence of a favorable pressure gradient of about $1/\rho\ (dp/dx) \sim 400$ cm/sec^2, or 20 times the analogous acceleration rate in the present experiment. It is anticipated then that the acceleration rate has to increase twenty folds to signficantly reduce the half-angle subtended by the spot.

The growth rates of spots generated in a decelerating boundary layer could not be visually observed, since the laminar flow surrounding the spot broke up due to the destabilizing effects of deceleration and the dye marking the spot became indistinguishable from the surrounding dye.

When the Blasius boundary layer was subjected to a uniform deceleration, a most interesting series of events was observed. Fluorescent dye seeped into the laminar boundary layer through the spanwise slot, and was illuminated by a horizontal sheet of laser light at $y = 0$. The thickness of the laser sheet was about 1 mm, several times the thickness of the undisturbed dye sheet. At a uniform speed of 40 cm/sec the boundary layer was Blasius. The dye sheet appeared smooth and uniform. The plate was then decelerated uniformly to a speed 30 cm/sec in 5 seconds. Two seconds after the deceleration had started, a two-dimensional wave pattern was evident. Alternating bright and dark bands of dye were evident, consistent with the passing of two-dimensional vorticity waves. The wavelength was about 5 boundary layer thicknesses as compared to 8δ for a Tollmien-Schlichting wave, and its phase speed relative to the plate was about 0.4 U_∞ as compared to 0.3 U_∞ for a Tollmien-Schlichting wave, where U_∞ is the terminal towing speed. The two-dimensional waves developed a three-dimensional pattern. This pattern evolved into several hairpin vortices characterized by the accumulation of dye in triangle-shaped regions. Since the thickness of the sheet of light is larger than the thickness of the undisturbed dye, lifting and accumulation of dye results in bright regions. The vortices appeared in several regular rows with a spanwise distance between two vortices of about 5 boundary layer thicknesses (the same as the wavelength of the two-dimensional waves). The patterns continued to convect towards the trailing edge of the plate, and new ones appeared near the leading edge. Side views of the hairpin vortices indicated that their heads moved away from the wall. When the vortex head reached a height of about half a boundary layer thickness, it then burst into turbulence. The turbulent regions grew in size and adjacent bursts coagulated. Shortly after, the dye pattern indicated turbulent flow over the entire plate.

The experiments where repeated with different initial velocities in the range 20 to 60 cm/sec and different deceleration rates in the range 1 to 60 cm/sec^2. The same sequence of events described above was observed in all runs. The length scales were not sensitive to the changes in the deceleration

rate. However, the time to complete the transition process was approximately inversely proportional to the deceleration rate. The stages of transition are summarized in the schematic depicted in Figure 4.

The Blasius boundary layer was also subjected to uniform acceleration. The visualization experiments revealed no apparent effect on the sheet of dye on the surface of the plate. The dye had the glassy uniform appearance characteristic of a laminar flow. This is consistent with the expected stabilizing effect of acceleration, analogous to a favorable pressure gradient.

3.3 Hot-Wire Measurements

Miniature hot-film probes were used to measure the instantaneous longitudinal velocity in the laminar, transitional and turbulent boundary layers. The probes were moved rigidly with the plate, so that all velocities recorded were relative to the plate. For a laminar boundary layer, the boundary layer was Blasius, indicating zero pressure gradient, as shown on Figure 5. The velocity profiles are plotted in the normal boundary layer coordinates, where the ambient speed U_o is used as a velocity scale and the length scale $\sqrt{\frac{\nu x}{U_o}}$ is proportional to the laminar boundary layer thickness δ. The Reynolds number for the two repeat runs shown in Figure 5 was 6.7×10^5. The solid line in the figure is a numerically generated Blasius profile.

A typical mean velocity profile in a turbulent boundary layer generated by tripping is shown in Figure 6. Here, the friction velocity u^* is used as a velocity scale, and the distance from the wall is expressed in wall units ν/u^*. The usual wall logarithic and wake regions are evident. The Reynolds number for the two repeat runs shown in Figure 6 was 1.0×10^6. Figure 7 shows the RMS turbulent intensities as function of the distance from the wall, for the same two runs shown in the previous figure. Here the outer variables U_∞ and δ are used for normalization. The results agree well with standard boundary layer results.

In a turbulent boundary layer, the burst detector yielded a value for the mean bursting frequency of 0.004 wall units (u^{*2}/ν) over a limited Reynolds number range in agreement with values in the literature. A histogram of the low-speed streak lengths revealed that the distribution was highly skewed, having a most probable duration of 10 wall units (ν/u^{*2}) and an average value of approximately 10% longer. Streaks were detected roughly three times more

often than bursts indicating that not all deterected streaks are associated with a turbulent burst.

The hot-film probes were also used to record the instantaneous longitudinal velocity during the deceleration of a laminar boundary layer. Figure 8 represents the instantaneous longitudinal velocity U(y) at $y/\delta = 0.1$, for a plate decelerated from an initial velocity $U_o = 40$ cm/sec to a final velocity $U_\infty = 32$ cm/sec in a time $t^* = 4.6$ seconds. The two arrows on the abscissa represent the starting and ending of deceleration. Initially, the flow is laminar and the velocity at this particular elevation is proportional to the towing speed. A short time† after the deceleration starts, a sinousiodal instability is observed. Its peak to peak amplitude grows fast. Characteristic turbulent fluctuations are then observed, followed by a return to the laminar state at the new towing speed. The turbulence, on the average, bring high speed fluid from outside the boundary layer to replace the low speed fluid near the wall.

A second probe at $y/\delta = 1$ recorded the signal shown in Figure 9. It is seen that the turbulent fluctuations, on the average, bring low speed fluid from the wall region to replace the high speed fluid at $y/\delta = 1$. Close inspection of the instability waves near the wall and away from the wall reveals that the two waves are out of phase, consistent with a spanwise vortical motion.

The probe measurements are consistent with the qualitative visualization experiments. The relaminization observed in the hot-film signal after the plate returns to a uniform speed does not show in the dye pictures, however, since the dye mixing is irreversible; a reminder of the difficulties of correctly interpreting dye visualization results.

3.4 Analogies Between Transitional and Turbulent Boundary Layers

An interesting observation from the present visualization and probe measurement experiments, as well as experiments conducted in other laboratories, is the apparent similarities between events in a transitioning boundary layer and the intermitten. events that take place in the wall region of a turbulent boundary

---

†The exact delay time between the start of deceleration and the onset of instability is difficult to determine, since the observed waves are infinitesimal at first.

layer. Whether the laminar boundary layer disturbances are initially two-dimensional, e.g., due to a vibrating ribbon or to deceleration, or are three-dimensional, e.g., as in Gaster and Grant (1975) experiments or in the region just external to a spot, a similar sequence of events is observed to occur. First, a locally inflectional profile develops, due to the initial disturbances. Then a three-dimensional disturbance occurs, characterized by a horseshoe vortex lift-off. Final remnants of the event appear as counter-rotating vortices near the wall. In turbulent boundary layers there is evidence for a similar sequence of events. Local, inflectional velocity profiles have been observed (Blackwelder and Kaplan, 1976), which appear to be followed by the lift-off of a horseshoe vortex. It is very possible that in the turbulent case counter-rotating vortices are left near the wall as the horseshoe votex lifts off and is advected downstream, and that these vortices 'pump' low speed fluid away from the wall, causing the low-momentum streaks observed in previous experiments.

The exact origin of the counter-rotating vortices in transional and turbulent boundary layers is presently unknown, except in the case of a boundary layer on a concave wall where Görtler instability is known to generate these vortices. There, the curvature induces a centrifugal force acting upon the fluid particles which is counter balanced by a pressure gradient normal to the wall. Instability will occur if, upon perturbing a fluid particle, the imposed pressure gradient is not sufficient to provide a restoring force greater than the centrifugal force (Görtler, 1941). Smith (1955) showed that the Görtler instability leads to a series of counter-rotating streamwise vortices near the concave wall.

There has been some speculation that the counter-rotating vortices observed during transition on a <u>flat</u> plate are caused by the same instability mechanism, where the Tollmien-Schlichting wave system causes a curvature of sufficient magnitude in the streamlines (Görtler & Witting, 1958). In the turbulent boundary layer, Coles (1978) speculated that the random background turbulence cause sufficient curvature in the instantaneous streamlines to trigger a Görtler instability leading to the creation of counter-rotating vortices. More recently, Blackwelder (1982) presented an elegant scaling argument to compare the structures observed in transitional and turbulent boundary layers. He used the velocity gradient at the wall and viscosity for determining a length scale and a velocity scale in both flow fields. Thus, the length scale is

$$\left\{\nu \Big/ \left(\frac{\partial U}{\partial y}\right)_o\right\}^{1/2} ,$$

and the velocity scale is

$$\left\{\nu \left(\frac{\partial U}{\partial y}\right)_o\right\}^{1/2} .$$

In a turbulent boundary layer, these scales are common and are referred to as wall units. However, the use of this scaling for a transitioning boundary layer is novel. When the structures observed in both flow fields are scaled with the appropriate wall units, Blackwelder reported striking similarities. This, together with our visual observations in a decelerating laminar boundary layer, in a turbulent region embedded in a laminar flow, and in a fully-developed turbulent boundary layer, provide further evidence for the similarities between transitional and turbulent boundary layers. Our understanding of turbulent boundary layers and our ability to manipulate the flows to achieve drag reduction, enhanced mixing, etc. will be greatly increased with further theoretical development that exploit these apparent similarities.

4. Summary

During the past four years experimental studies of transitional and turbulent boundary layers have been conducted on flat plates in the 18 meter towing tank. During the early phases of this investigation, a flat plate developed for earlier studies was utilized. To improve the experimental configuration and to develop the ideas discussed below, a second plate was constructed in a modular form. This allowed different types of dye injection slots to be utilized at variable distances downstream of the leading edge. The modular plate was constructed of plexiglas mounted on a honeycomb section. The entire model was neutrally buoyant, thus preventing the middle of the plate from sagging under its own weight. The last portion of the experiment utilized a third flat plate model which incorporated the previous advances and also had an insert section for changing and testing localized surfaces and incorporated an improved probe support and traverse system.

Turbulent spots were studied to illuminate the nature of their growth within an unstable laminar boundary layer. The turbulent boundary layer was also investigated to understand more of its dynamics and to compare it with the growth and destabilization mechanism found earlier in the spot.

Our earlier work had suggested that turbulent spots developing in a laminar boundary layer grew in the spanwise direction by a destabilization mechanism. To explore this idea further three new visualization techniques were utilized. Instead of injecting a dye sheet, a series of dye lines were used. A better visualization of the three-dimension motion was obtained because the motion of the dye lines in the spanwise direction was clearly visible whereas uniform dye sheets obscured this motion. Before the laminar layer becomes turbulent, oscillations of the individual dye lines are observed as seen in Figure 4 of Gad-el-Hak, et al. (1981). Although the oscillations often appeared to be waves, their wavelengths are of the order of the boundary layer thickness and thus cannot be Tollmien-Schlichting waves. Several characteristics, such as their short wavelength and localized nature, suggest these disturbances are more closely related to the breakdown oscillations observed by Klebanoff, et al. (1962) following the nonlinear growth of Tollmien-Schlichting waves.

To determine if these oscillations were correlated with and/or possibly imposed by turbulence within the spot at a higher elevation above the wall, an oscillator was constructed which displaced the illuminating sheet of laser

light from $y = 0$ to $y = \delta$. These two elevations could be alternatively seen at a rate of approximately 48 cycles/sec. The high oscillation rate allowed the two planes to be viewed almost simultaneously; i.e. with time separations that were small compared to the time scales of the turbulent spot. Movie films revealed that the turbulent region at $y = \delta$ extended far upstream of the simultaneous turbulence at the wall. This phenomenon, called an overhang, had been previously documented along the centerline of the spot by different investigations using hot-wire or laser anemometers. However, our films showed that the same phenomenon occurred everywhere along the leading edges of the spot and it appeared everywhere simultaneously; i.e. it was not occurring at random or in an oscillating mode. Furthermore, the oscillations at the wall only occurred whenever there was an overhang at $y = \delta$ suggesting that the outer turbulence does indeed trigger the oscillating motion at the wall.

The localized transition to turbulence was also briefly explored by using a brine dye laid on the plate before towing began. The dye was heavier than the surrounding fluid and was only removed slowly by the laminar flow. However, when a spot passed by, the vigorous turbulent action rapidly mixed the dye with the surrounding fluid. Thus the brine dye provided a convenient means of observing the laminar-turbulent transition process on the plate. As the turbulent spot drew near, definite imprints within the laminar flow could be observed. Presumably this was imposed from the overhang structure in agreement with the previous results.

Visualization of the low speed streaks in the wall region of turbulent boundary layers has also been attempted using fluorescent dye and thin sheets of laser light. Since the streaks inhabit only the region $0<y^+<30$, i.e. $0<y<1.5$ mm in the towing tank, they are difficult to visualize. The large number of variables in the visualization process, e.g. thickness of the light sheet, height of the sheet above the wall, location of the injection slot, have made repeatability of problem. Nevertheless, the low speed streaks have been observed for distances up to 3 cm downstream of the injection slot before breaking up into turbulence.

Recently a new visualization technique, borrowed from Carlson, et al. (1981), has been attempted with extremely promising initial results. Mica platelets, having a thickness of 2-5 micron and a diameter of 10-20 micron, and coated with titanium dioxide, were injected through the dye slots.

Because of their extremely small and flat shape, they tend to align themselves with the instantaneous shear in the fluid. Elongated patterns were observed downstream of the dye slot before turbulent mixing completely randomized the patterns. This mode of visualization clearly produced a different representation and view of the flow field than dye. The elongated patterns associated with the streaky wall structure could be observed 10-12 cm downstream of the slot compared to only 3 cm for the dye. Presumably this resulted from the platelets responding more to the instantaneous shear rather than to an integrated diffusion effect. It is expected that this technique will be invaluable whenever wave patterns are present such as in the decelerating boundary layer.

Hot-film sensors and anemometers were utilized to document the laminar and turbulent boundary layers and provide data for advanced analysis. The anemometer signals were digitized, stored on a magnetic disc and analyzed via FORTRAN programs. The velocity profiles in the laminar boundary layer agreed with the Blasius solutions extremely well, i.e. with a scatter less than 5%, over the entire plate.

When trips were installed to form a turbulent boundary layer, the measured mean velocity profile displayed the usual wall, logarithmic and wake regions. The friction velocity and skin friction coefficient were obtained from the slope of the logarithmic zone and agreed well with standard boundary layer results. The rms velocity profile, u'(y), also compared well with existing data.

A burst detection process was implemented using a digital algorithm similar to that of Blackwelder and Kaplan (1976). The mean bursting frequency was measured to be approximately $0.004\ u^{*2}/\nu$ over a limited Reynolds number range in agreement with values in the literature.

A new algorithm was developed to detect the low speed streaks as they passed a rake of three hot-film sensors. The probes were located $10\ \nu/u^*$ above the plate at the same streamwise position with a spanwise separation of approximately $20\ \nu/u^*$. Thus the total array spanned $40\ \nu/u^*$ which is approximately half the average low speed streak spacing. The detection algorithm was designed to detect the low speed streaks by searching for two characteristics of the streaks, namely for those regions where (1) the velocity on the center probes was less than u' below the mean value and the two outer probes were less than 0.5 u' below the mean and (2) the curvature of the

instantaneous profile U(z) was negative. A histogram of the streak lengths revealed that the distribution was highly skewed, having a most probable duration of 10 ν/u^{*2} and an average value approximately 10% longer. Streaks were detected roughly three times more often than bursts indicting that not all detected streaks are associated with a turbulent burst.

The results of the algorithm were compared with iso-velocity contours obtained from a rake having a wider spanwise extent. The comparison showed that the detection picked out the streaks exceedingly well and secondly that the streaks meander in the spanwise direction so that often a single streak crosses the probes two or more times resulting in multiple detections. Correspondingly, the true length of the streaks are longer than the values given above.

The effects of acceleration and deceleration on turbulence and transition were investigated experimentally and numerically. Two flow fields were considered; turbulent spots and unstable laminar boundary layers. Turbulent spots growing in laminar boundary layers were subjected to uniform acceleration and deceleration in the range 1 to 60 cm/sec^2. The acceleration tended to stabilize the flow, and the half-angle subtended by the spot was slightly reduced. Acceleration rates much higher than the one achieved in the present experiments are probably needed to significantly reduce the growth rate of turbulent spots. The deceleration resulted in the destabilizaton of the boundary layer, in a way that rendered the original turbulent spots indistinguishable from the surrounding fluid. Sophisticated pattern recognition techniques will help in isolating the artifically triggered spot and enable us to measure its growth under different deceleration conditions. It is anticipated that deceleration would increase the growth rates of turbulent spots.

A Blasius boundary layer subjected to uniform deceleration underwent a well-defined route to complete transition. The visualization experiments revealed the onset of two-dimensional waves that appeared after the deceleration had started, three-dimensionality was then apparent and led to the formation of hairpin vortices that lifted away from the wall and burst into turbulence.

The formation and growth of the vorticity waves in the decelerating laminar boundary layer were also observed using hot-film probes. The probes were moved with the plate, and indicated high speed (relative to the plate) fluid coming from the outerparts of the ambient fluid towards the wall region. The probes also indicated a return to the laminar state after the deceleration ceased.

For the decelerating flat plate, the boundary layer equations were linearized and appropriate similarity variables were introduced. The resulting initial value problem was solved numerically using a Crank-Nicholson implicit scheme. The resulting velocity profiles were inflectional, with the inflection point initially at the wall, moving upward on a diffusion time scale and finally going back to the wall. The inflectional profiles are less stable than Blasius, and this probably governs the onset of instability observed in the present investigation.

The above numerical results are only qualitatively correct because of the linearization. The nonlinear, unsteady boundary layer equations should be solved numerically, and the stability of the resulting profiles should be investigated. It is expected that this calculation will yield a 'most dangerous' profile that will explain the delay time between the start of deceleration and the onset of instability observed in the present experiment.

Further probe measurements are needed to determine the 'degree' of two-dimensionality of the vorticity waves observed in the decelerating plate experiments. If the waves are truly two-dimensional, it suggests the study of their instability in order to determine the mechanism and characteristics of the development of three-dimensionality. If there is a well-defined transition from laminar two-dimensional waves to laminar three-dimensional waves through an instability process, one has identified a major link in the transition process. An understanding of this instability would allow one to contemplate means of interferring with the process to delay transition or reinforcing the process to foster transition. This will be useful in numerous engineering applications.

The work on the stability of accelerating and decelerating <u>laminar</u> boundary layers is a step toward understanding the more complicated problem of the effects of acceleration or deceleration on <u>turbulent</u> boundary layers. This problem has obvious relevance in accelerating or decelerating vehicles, vehicles experiencing turn and other maneuvers, rotating propellers, and many other practical situations.

On a more basic side, the acceleration/deceleration offer a convenient way to modulate laminar and turbulent boundary layers to determine the exact nature of the apparent analogies between the different transition events in a laminar boundary layer and the intermittent events that characterize fully-developed

turbulent boundary layers, namely the bursting cycle. We have presented visual evidence of this analogy. Blackwelder (1982) presented scaling arguments to show the similarities between turbulent and transitional flow fields. Further theoretical development that exploit these apparent similarities are needed.

References

Anders, J. B., and R. F. Blackwelder (1979) "Longitudinal Vortices in a Transitioning Boundary Layer," Proc. IUTAM Symp. on Laminar-Turbulent Transition, Springer-Verlag, p. 110.

Blackwelder, R. F. (1982) "Analogies Between Transitional and Turbulent Boundary Layers," Submitted to Phys. Fluids.

Blackwelder, R. F., and H. Eckelmann (1979) "Streamwise Vortices Associated with the Bursting Phenomenon," J. Fluid Mech., Vol. 94, p. 577.

Blackwelder, R. F., and R. E. Kaplan (1976) "On the Wall Structure of the Turbulent Boundary Layer," J. Fluid Mech., Vol. 76, p. 89.

Burgers, J. M. (1924) "The Motion of a Fluid in the Boundary Layer Along a Plane Smooth Surface," Proc. 1st Int. Cong. of Applied Mech., Delft, p. 113.

Cantwell, B., D. Coles, and P. Dimotakis (1978) "Structure and Entrainment in the Plane of Symmetry of a Turbulent Spot," J. Fluid Mech., Vol. 87, p. 641.

Carlson, D. R., S. E. Widnall, and M. F. Peeters (1981) "A Flow Visualization Study of Transition in Plane Poiseuille Flow," Fluid Dyn. Research Lab. Report No. 81-3, Mass. Inst. Technology.

Charters, A. C. (1943) "Transition Between Laminar and Turbulent Flow by Transverse Contamination," N.A.C.A. Tech. Note No. 891.

Coles, D. (1978) "A Model for Flow in the Viscous Sublayer," in Coherent Structures of Turbulent Boundary Layers, edited by C. R. Smith and D. E. Abbott, Lehigh Univ., p. 462.

Coles, D., and S. J. Barker (1975) "Some Remarks on a Synthetic Turbulent Boundary Layer," in Turbulent Mixing in Nonreactive and Reactive Flows, edited by S. N. B. Murthy, Plenum, p. 285.

Corrsin, S., and A. L. Kistler (1955) "Free-Stream Boundaries of Turbulent Flows," N.A.C.A. Report No. 1244. (Supersedes N.A.C.A. TN 3133.)

Davis, S. H. (1976) "The Stability of Time-Periodic Flows," Ann. Rev. Fluid Mech., Vol. 8, p. 57.

Davis, S. H., and M. Gad-el-Hak (1981) "Transition in Decelerating Boundary Layers," Bull. Amer. Phys. Soc., Vol. 26, p. 1251.

Drazin, P., and W. Reid (1981) Hydrodynamic Stability, Cambridge University Press.

Dryden, H. L. (1934) "Boundary Layer Flow Near Flat Plates," Proc. 4th Int. Cong. of Applied Mech., Cambridge, England, p. 175.

Dryden, H. L. (1936) "Airflow in the Boundary Layer Near a Plate," N.A.C.A. Report No. 562.

Dryden, H. L. (1939) "Turbulence and the Boundary Layer," J. Atmos. Sci., Vol. 6, p. 85.

Elder, J. W. (1960) "An Experimental Investigation of Turbulent Spots and Breakdown to Turbulence," J. Fluid Mech., Vol. 9, p. 235.

Emmons, H. W. (1951) "The Laminar-Turbulent Transition in a Boundary Layer," J. Aero Sci., Vol. 18, p. 490.

Falco, R. E. (1978) "The Role of Outer Flow Coherent Motions in the Production of Turbulence Near a Wall," in Coherent Structures of Turbulent Boundary Layers, edited by C. R. Smith and D. E. Abbott, Lehigh Univ., p. 448.

Gad-el-Hak, M., R. F. Blackwelder, and J. J. Riley (1980) "A Visual Study of the Growth and Entrainment of Turbulent Spots," Proc. IUTAM Symp. on Laminar-Turbulent Transition, Springer-Verlag, p. 297.

Gad-el-Hak, M., R. F. Blackwelder, and J. J. Riley (1981) "On the Growth of Turbulent Regions in Laminar Boundary Layers," J. Fluid Mech., Vol. 110, p. 73.

Gaster, M. (1975) "A Theoretical Model of a Wave Packet in the Boundary Layer on a Flat Plate," Proc. Roy. Soc. A, Vol. 347, p. 271.

Gaster, M. (1978) "The Physical Processes Causing Breakdown to Turbulence," 12th Naval Hydrodynamics Symposium, Washington, D.C., p. 22.

Gaster, M., and I. Grant (1975) "An Experimental Investigation of the Formation and Development of a Wave Packet in a Laminar Boundary Layer," Proc. Roy. Soc. A, Vol. 347, p. 253.

Görtler, H. (1941) "Über eine dreidimensionale Instabilität laminarer Grenzschichten an konkaven Wänden," ZAMM, Vol. 21, p. 250.

Görtler, H., and H. Witting (1958) "Theorie der Sekundären Instabilität der Laminaren Grenzschichten," IUTAM Symp. on Boundary Layer Research, edited by H. Görtler, Springer-Verlag, p. 110.

Hama, F. R., J. D. Long, and J. C. Hagarety (1957) "On Transition from Laminar to Turbulent Flow," J. Appl. Phys., Vol. 28, p. 388.

Klebanoff, P. S., K. D. Tidstrom, and L. M. Sargent (1962) "The Three-Dimensional Nature of Boundary Layer Instability," J. Fluid Mech., Vol. 12, p. 1.

Kovasznay, L. S. G., H. Komoda, and B. R. Vasudeva (1962) "Detailed Flow Field in Transition," Proc. Heat Transfer and Fluid Mech. Inst., Stanford University Press, p. 1.

Lin, J.-T., and Y.-H. Pao (1979) "Wakes in Stratified Fluids," Ann. Rev. Fluid Mech., Vol. 11, p. 317.

Meyer, K. A., and S. J. Kline (1961) "A Visual Study of the Flow Model in the Later Stages of Laminar-Turbulent Transition on a Flat Plat," Mech. Eng. Dept., Stanford University, Report No. MD-7.

Morkovin, M. V. (1969) "Critical Evaluation of Transition from Laminar to Turbulent Shear Layers with Emphasis on Hypersonically Travelling Bodies," Flight Dyn. Lab., Report No. AFFDL-TR-68-149.

Rosenhead, L. (1963) Laminar Boundary Layers, Oxford Clarendon Press.

Schlichting, H. (1933) "Zur Entstehung der Turbulenz bei der Plattenströmung," Z. angew. Math. Mech., Vol. 13, p. 171.

Schlichting, H. (1968) Boundary Layer Theory, McGraw-Hill.

Schubauer, G. B., and P. S. Klebanoff (1956) "Contributions on the Mechanics of Boundary Layer Transition," N.A.C.A. Report No. 1289.

Schubauer, G. B., and H. K. Skramstad (1948) "Laminar Boundary Layer Oscillations on a Flat Plate," N.A.C.A. Report No. 909.

Smith, A. M. O. (1955) "On the Growth of Taylor-Görtler Vortices Along Highly Concave Walls," Quart. Appl. Math., Vol. 13, p. 233.

Squire, H. B. (1933) "On the Stability of Three-Dimensional Disturbances of Viscous Flow Between Parallel Walls," Proc. Roy. Soc. A, Vol. 142, p. 621.

Stewartson, K. (1951) "On the Impulsive Motion of a Flat Plate in a Viscous Fluid," Quat. J. Mech., Vol. 4, p. 182.

Tollmien, W. (1931) "The Production of Turbulence," N.A.C.A. TM 609.

Townsend, A. A. (1976) The Structure of Turbulent Shear Flow, Cambridge University Press.

Van Atta, C. W., and K. N. Helland (1980) "Exploratory Temperature-Tagging Measurements of Turbulent Spots in a Heated Laminar Boundary Layer," J. Fluid Mech., Vol. 100, p. 243.

Van der Hegge Zijnen, B. G. (1924) "Measurements of the Velocity Distribution in the Boundry Layer Along a Plane Surface," Thesis, Delft.

Wygnanski, I. (1980) "The Effects of Reynolds Number and Pressure Gradient on the Transitional Spot in a Laminar Boundary Layer," Proc. of the Meeting on Structure of Turbulence and Mixing, Madrid, Spain, Springer.

Wygnanski, I., M. Sokolov, and D. Friedman (1976) "On a Turbulent 'Spot' in a Laminar Boundary Layer," J. Fluid Mech., Vol. 78, p. 785.

Zilberman, M., I. Wygnanski, and R. E.Kaplan (1977) "Transitional Boundary Layer Spot in a Fully Turbulent Environment," Phys. Fluids Suppl., Vol. 20, p. 258.

Appendix I: Conventional Statistics

```
******** PROGRAM TO COMPUTE THE CONVENTIONAL STATISTICS                    PAGE 0001

    1) C ********** PROGRAM TO COMPUTE THE CONVENTIONAL STATISTICS
    2) C               AND STORE THE RESULTS IN AN INFORMATION BLOCK
    3) C
    4)       PARAMETER (LEN=11)
    5)       REAL A(32),UBAR(LEN),RMS(LEN),C(4,LEN),B(128)
    6)       REAL*8 SUMU(LEN),SUMSQ(LEN)
    7)       REAL*8 AA,BB
    8)       CHARACTER *32 FNAME
    9)       CHARACTER *5 RUNO
   10)       INTEGER*4 KCHN(5),LCHN(32)
   11)       INTEGER*2 IU(4096)
   12)       DATA SUMU/LEN*0./,SUMSQ/LEN*0./,UBAR/LEN*0./,RMS/LEN*0./
   13) C
   14) C ********** READ INDX FILE
   15) C
   16)       PRINT *,'ENTER LAST FIVE CHARACTERS OF RUN NAME'
   17)       READ(1,'(A5)') RUNO
   18)       FNAME='INDX/COAT'//RUNO
   19) C     PRINT *,' FILE NAME IS ',FNAME
   20)       OPEN(40,FILE=FNAME,STATUS='OLD',RECL=256,ERR=5,
   21)      *FORM='UNFORMATTED',ACCESS='DIRECT')
   22)       READ(40,ERR=5) (IU(K),K=1,256)
   23)       CLOSE(40)
   24)       KCHN(1) = IU(181)       /*TOTAL NUMBER OF CHANNELS RECORDED
   25)       IF(KCHN(1).GT.LEN) STOP 'PROGRAM ONLY ACCEPTS 11 CHANNELS'
   26)       KCHN(2) = IU(182)       /*1ST CHN OF ADC'S USED
   27)       CALL RN2P(IU(9),DT,INTL(1))
   28)       WRITE(1,3) DT
   29) 3     FORMAT(/,' DIGITIZING INTERVAL =',F8.5,' SECONDS.',/)
   30)       A(21) = DT                          /*DIGITIZING INTERVAL
   31)       CALL RN2P(IU(159),U00,INTL(1))
   32)       WRITE(1,4) U00
   33) 4     FORMAT(' RECORDED VALUE OF U00 =',F6.1,' CM/SEC.',/)
   34)       A(22) = U00
   35)       GO TO 10
   36) 5     PRINT *,' ERROR ENCOUNTERED IN READING',FNAME
   37) C
   38) C ******** READ THE COEFFICIENT FILE
   39) C
   40) 10    FNAME='COEF/COAT'//RUNO
   41) C     PRINT *,' COEFFICIENT FILE IS ',FNAME
   42)       OPEN(31,FORM='UNFORMATTED',STATUS='OLD',FILE=FNAME)
   43)       READ(31) B
   44)       CALL RN2P(B,B,INTL(128))
   45)       CLOSE(31)
   46)       IC=4*KCHN(2)     /*BIAS COEF TO FIRST CHAN RECORDED
   47)       DO 20 K = 1,KCHN(1)
   48)       LCHN(K)=K+KCHN(2)-1
   49)       DO 20 J = 1,4
   50)       IC = IC + 1
   51) 20    C(J,K) = B(IC)
   52)       PRINT *,' CHANNEL        A          B          C          D'
   53)       WRITE(1,23) (LCHN(L),(C(J,L),J=1,4),L=1,KCHN(1))
```

******** PROGRAM TO COMPUTE THE CONVENTIONAL STATISTICS PAGE 0002

```
   54) 23    FORMAT(I5,6X,4G10.3)
   55) C
   56) C ******** INPUT CHANNEL NUMBER OF HOT-FILMS
   57) C
   58)       PRINT *,'TOTAL NUMBER OF CHANNELS RECORDED =',KCHN(1)
   59)       CALL TNOUA(' ENTER CHANNEL NUMBER OF FIRST HOT-FILM:  ',42)
   60)       READ(1,*) KCHN(3)
   61)       CALL TNOUA(' ENTER TOTAL NUMBER OF HOT-FILMS RECORDED:  ',44)
   62)       READ(1,*) KCHN(4)
   63)       IFILM = KCHN(4)
   64) C
   65) C ********** SELECT THE TIME INTERVAL TO ANALYSE
   66) C
   67)       RECL = INT (4096/KCHN(1))*DT /*RECORD LENGTH IN SECONDS
   68)       CALL TNOUA(' ENTER THE STARTING TIME[SEC]:  ',32)
   69)       READ(1,*) TSTART
   70)       ISTART = TSTART/RECL+1
   71)       TSTART =(ISTART-1)*RECL +DT
   72)       PRINT *,'TSTART =',TSTART
   73)       CALL TNOUA(' ENTER THE STOPPING TIME[SEC]:  ',32)
   74)       READ(1,*) TSTOP
   75)       ISTOP = TSTOP/RECL+1
   76)       TSTOP =ISTOP * RECL
   77)       PRINT *,'TSTOP =',TSTOP
   78) C
   79) C *********** COMPUTE THE MEAN AND RMS VALUES OF ALL CHANNELS
   80) C
   81)       FNAME='DATA/COAT'//RUNO
   82)       ICH = KCHN(1)
   83)       C2V=1./409.6
   84)       C2V2=C2V*C2V
   85)       C2V3=C2V2*C2V
   86)       JBLK = 0
   87)       IBA = 0
   88)       LRCL=(4096/ICH)*ICH
   89)       OPEN(29,FORM='UNFORMATTED',STATUS='OLD',FILE=FNAME,ERR=901)
   90)    40 READ(29,END=110,ERR=902) IU
   91)       JBLK = JBLK + 1
   92)       IF(JBLK.LT.ISTART) GO TO 40
   93)       IF(JBLK.GT.ISTOP) GO TO 40
   94) C     WRITE(1,11) (IU(M),M=1,LEN)
   95) 11    FORMAT(5I9)
   96) C        ADD THE PRESENT DATA TO THE SUMMED STATISTICS
   97)       IBA = IBA + 1
   98)       DO 55 K=KCHN(3),KCHN(3)+KCHN(4)-1
   99)       AA=0.D0
  100)       BB=0.D0
  101)       COF1=C(1,K)
  102)       COF2=C(2,K)*C2V
  103)       COF3=C(3,K)*C2V2
  104)       COF4=C(4,K)*C2V3
  105)       DO 50 J=K,LRCL,ICH
  106)       V=FLOAT(IU(J))
```

********* PROGRAM TO COMPUTE THE CONVENTIONAL STATISTICS PAGE 0003

```
      U=COF1+V*(COF2+V*(COF3+V*COF4))
      AA=AA+U
   50 BB=BB+U*U
      SUMU(K)=SUMU(K)+AA
   55 SUMSQ(K)=SUMSQ(K)+BB
    C PRINT *,' FINISHING ',JBLK,' PASS'
      GO TO 40
    C
    C ******** NORMALIZE THE DATA
    C
  110 CLOSE(29)
      NORM = 4096/ICH
      XNORM = IBA*NORM                    /*NORMALIZATION FACTOR
      DO 200 K = KCHN(3),KCHN(3)+KCHN(4)-1
      UBAR(K) = SUMU(K)/XNORM
      XX = SUMSQ(K)/XNORM
      IF(XX - UBAR(K)**2) 190,195,195
  190 PRINT *,' NEGATIVE SQRT ON THE',LCHN(K),' CHANNEL ==> RMS=0 '
      RMS(K) = 0.
      GO TO 200
  195 RMS(K) = DSQRT(SUMSQ(K)/XNORM - UBAR(K)**2)
  200 CONTINUE
    C
    C ******** OUTPUT THE DATA
    C
      A(23) = JBLK
      A(24) = ISTART
      A(25) = ISTOP
      OPEN(32,FILE='BURST.DATA'//RUNO,FORM='UNFORMATTED')
      WRITE(32)A,C,UBAR,RMS,KCHN,FNAME     /*WRITE INFORMATION ONTO DISK
      CLOSE(32)
      TREC = RECL*IBA
      XREC = RECL*JBLK
      WRITE(1,209) TREC,XREC
  209 FORMAT(/,' THE MEAN STATISTICS FOR',F6.1,' SEC OF DATA ARE: '
     *,/,5X'(THE TOTAL AVAILABLE RECORD IS',F6.1,' SEC )')
      WRITE(1,211) (LCHN(J),UBAR(J),RMS(J),J=1,ICH)
  211 FORMAT(/,3X,'CHANNEL #   UBAR',9X,'RMS',/,12(4X,I7,2F12.2,/))
      CALL EXIT
    C 901 DATA FILE OPEN ERROR
    C 902 DATA FILE READ ERROR
  901 STOP 901
  902 STOP 902
      END
```

Appendix II: Streaks Detector

PROGRAM (STREAK) JUNE 30, 1981 PAGE 0001

```
 1) C     RON4 PROGRAM (STREAK)                              JUNE 30, 1981
 2) C ******** COMPUTES THE LOCATIONS OF LOW SPEED REGIONS FROM THE 3
 3) C                SPANWISE HOT-FILMS USING THE SECOND DERIVATIVE OF
 4) C                DU/DZ OR A THRESHOLD ON THE VELOCITY DATA AND
 5) C                PLOTS THE HISTROGRAM OF THE STREAK LENGTHS.
 6) C                THIS PROGRAM ASSUMES THE MEAN AND RMS STATISTICS
 7) C                HAVE BEEN CALCULATED AND STORED ON THE DISK.
 8) C ----> CHANGING 'LENH' VARIES THE ABSCISSA OF THE HISTOGRAM
 9) C ----> 'XAM' CONTROLS THE NOMALIZATION OF THE HISTOGRAM ORDINATE.
10) C
11)       PARAMETER (LEN=11)
12)       PARAMETER (LENH=60)
13)       REAL A(32),UBAR(LEN),RMS(LEN),C(4,LEN),B(128),OLDT,NOWT
14)       REAL UB(4096),U(3),UT(3)
15)       INTEGER*2 IU(4096),HIST(LENH),ICH(3)
16)       INTEGER*4 ITOT,ISAV,KCHN(5)
17)       CHARACTER AST,BLNK,LINE(60)
18)       CHARACTER*32 FNAME
19)       CHARACTER*5 RUNO
20)       DATA AST/'*'/,BLNK/' '/,LINE/60*'-'/,HIST/LENH*0/
21) C
22) C ******** READ IN STORED INFORMATION FROM THE DISK
23) C
24)       PRINT *,' ENTER LAST FIVE CHAR OF RUN NAME : '
25)       READ(1,'(A5)') RUNO
26)       OPEN(32,FILE='BURST DATA'//RUNO,FORM ='UNFORMATTED',
27)      *      STATUS='OLD')
28)       READ(32) A,C,UBAR,RMS,KCHN,FNAME        /* INPUT STORED INFORMATION
29)       CLOSE(32)
30) C
31) C ******** SELECT THE 3 CHANNELS FOR THE STREAK ANALYSIS
32) C
33)       IF(KCHN(4) GT 2) GO TO 5
34)       PRINT *,' LESS THAN 3 CHANNELS OF H.F. RECORDED !!!'
35)       STOP
36)  5    WRITE(1,6) KCHN(3)
37)  6    FORMAT(' THE FIRST H.F  SIGNAL IS ON CHANNEL #',I3,'.')
38)       CALL TNOUA(' ENTER CHANNEL # OF FIRST H.F. TO ANALYSE : ',43)
39)       READ(1,*) ICH(1)
40)       ICH(2) = ICH(1) + 1          /* ASSUMES H.F. CHANNELS ARE SEQUENTIAL
41)       ICH(3) = ICH(1) + 2          /* ASSUMES H.F. CHANNELS ARE SEQUENTIAL
42)       PRINT *,' THE STREAK DETECTION WILL USE CHANNELS : ',ICH
43) C
44) C ******** SET UP PARAMETERS FOR DETECTING THE STREAKS
45) C
46)       NCH = KCHN(1)                /* TOTAL # OF CHANNELS RECORDED
47)       RECL=INT(4096/NCH)*A(21)        /* A(21)=DT
48)       THRES = 1.                   /* THRESHOLD USED FOR VELOCITY
49)       DO 10 K = 1,3
50) 10    ICH(K) = ICH(K)-KCHN(2)+1    /* BIAS ICH TO 1ST CHANNEL INDEX
51)       UT(1) = UBAR(ICH(1)) - 0.5*THRES*RMS(ICH(1))  /* VELOCITY THRESHOLD
52)       UT(2) = UBAR(ICH(2)) - 1.0*THRES*RMS(ICH(2))  /* VELOCITY THRESHOLD
53)       UT(3) = UBAR(ICH(3)) - 0.5*THRES*RMS(ICH(3))  /* VELOCITY THRESHOLD
```

PROGRAM (STREAK) JUNE 30, 1981 PAGE 0002

```
      ITOT = 0                        /* TIME COUNTER
      OLDT = 0.                       /* STATUS WORD OF PREVIOUS DATA POINT
      NOWT = 0.                       /* STATUS WORD OF PRESENT DATA POINT
      GAMMA = 0.
      IT = 0                          /* COUNTS NUMBER OF STREAKS
      DT = A(21)                      /* DIGITIZING INTERVAL
      UOO = A(22)                     /* TOWING SPEED
      NBLK = A(23)                    /* TOTAL # OF (4096) BLOCKS OF DATA
      ISTART = A(24)                  /* ISTART=FIRST BLOCK OF DATA TO ANALYSE
      ISTOP = A(25)                   /* ISTOP=LAST BLOCK OF DATA TO ANALYSE
      CALL TNOUA(' ENTER THE VALUE OF UTAU(CM/SEC) : ',34)
      READ(1,*) UTAU
      PRINT *,'STREAK STARTING TIME     STREAK STOPPING TIME'
C
C ******** BEGIN MAIN LOOP
C
      IBLK = NBLK
      LBLN = (4096/NCH)*NCH
      OPEN(29,FORM='UNFORMATTED',STATUS='OLD',FILE=FNAME)
      DO 210   IB = 1,IBLK
      READ(29,ERR=901)  IU
      IF(IB.LT.ISTART) GO TO 210
      IF(IB.GT.ISTOP) GO TO 210
      CALL LINEAR3(IU,UB,C,ICH(1),NCH)
      DO 200 J = ICH(1),LBLN,NCH
      ITOT = ITOT + 1
      DO 30 K = 1,3
30    U(K) = UB(J+K-1)
      CR = U(3) - 2.*U(2) + U(1)     /* C = CURVATURE = 2ND DERIVATIVE
      IF(CR) 35,35,40              /* IF C>0 ==>MINIMUM==>POSSIBLY STREAK
35    IF(U(1) - UT(1)) 38,38,150    /* STRONG DEFECT==>STREAK
38    IF(U(3) - UT(3)) 40,40,150    /* STRONG DEFECT==>STREAK
40    IF(U(2) - UT(2)) 60,60,150    /* STRONG DEFECT==>STREAK
C
C ******** STATEMENT 60==> THERE IS A SLOW SPEED REGION
C
60    NOWT = 1.
      GAMMA = GAMMA + 1.
      IF(OLDT.EQ.NOWT) GO TO 200
C ******** THIS IS A NEW LOW SPEED REGION
      DUMIB=IB
      DUMJ=J
      T1=((DUMIB-1.)+((DUMJ-1.)/4096.))*RECL
      IT = IT + 1
      ISAV = ITOT
      GO TO 190
C
C ******** STATEMENT 150==> THERE IS NO LOW SPEED REGION
C
150   NOWT = 0.
      IF(OLDT.EQ.NOWT) GO TO 200
C ******** THIS IS THE END OF THE LOW SPEED REGION
      DUMIB=IB
```

PROGRAM (STREAK) JUNE 30, 1981 PAGE 0003

```
      DUMJ=J
      T2=((DUMIB-1.)+((DUMJ-1.)/4096.))*RECL
      WRITE(1,'(2(5X,F8.4))') T1,T2
      LPOS = ITOT - ISAV
      IF(LPOS.GT.LENH) LPOS = LENH
      HIST(LPOS) = HIST(LPOS) + 1
190   OLDT = NDWT
200   CONTINUE
210   CONTINUE
      CLOSE(29)
C
C ******** COMPUTE THE MEAN STATISTICS
      TREC = ITOT*DT                    /* TOTAL RECORD LENGTH
      PLS = UTAU*UTAU/0.01              /* NORMALIZING CONSTANT
      IF(IT .EQ. 0)  WRITE(1,220)
      IF(IT .EQ. 0)  GO TO 901
220   FORMAT(' ****  NO STREAKS WERE DETECTED  **** ')
      ALNGTH = GAMMA*DT/IT*PLS          /* AVERAGE LENGTH IN T+
      GAMMA = GAMMA/ITOT*100.           /* INTERMITTENCY FACTOR
      FREQ = IT/TREC                    /* FREQUENCY
      FPLS = FREQ/PLS                   /* F+
      WRITE(1,251) RUNO, IT, TREC, GAMMA, FREQ, FPLS, ALNGTH
251   FORMAT(///,10X,'FOR RUN # ',A5,', ',I5,' STREAKS',
     *' WERE FOUND IN A',/,15X,'TOTAL RECORD OF',F7.2,
     *'SECONDS ',/,20X,'GAMMA      =',F8.2,'%',/,20X
     *,'FREQUENCY =',F7.1,' HZ',/,20X,'F+',8X,'=',F8.4,/
     *,20X,'LENGTH T+ =',F8.1,/)
C
C ******** FIND THE MAXIMUM IN THE HISTOGRAM
C
      MAX = 0
      DO 300 I = 1,LENH
      IF(HIST(I).LT.MAX) GO TO 300
      MAX = HIST(I)
300   CONTINUE
340   XAM = FLOAT(MAX)/60.
C     XAM = 1.                          /* XAM = 1. ==>UNNORMALIZED HISTOGRAM
C
C ******** PLOT THE HISTOGRAM
C
      DO 520 I = 1,60
520   LINE(I) = '-'
      WRITE(1,551) LINE                 /* PRINT THE ORDINATE AXIS
551   FORMAT(//,11X,6(9X,':'),/,' LEN      #   ',60A1)
      DO 560 J = 1,60
560   LINE(J) = BLNK                    /* ZERO THE LINE ARRAY
      DO 600 I = 1,LENH
      STL = I*DT*PLS                    /* STREAK LENGTH IN T+
      JH = HIST(I)/XAM + 0.5            /* JH = SCALED ORDINATE OF HISTOGRAM
      IF(JH.NE.0) GO TO 575
      WRITE(1,566) STL,HIST(I)          /* OUTPUT HISTOGRAM IF JH=0
566   FORMAT(F5.1,I4,'  :')
      GO TO 600
```

PROGRAM (STREAK) JUNE 30, 1981 PAGE 0004

```
160) 575   IF(JH GT 60) JH = 60
161)       DO 580 J = 1,JH
162) 580   LINE(J) = AST                    /* PLACE '*' INTO LINE ARRAY
163)       WRITE(1,581) STL,HIST(I),LINE    /* OUTPUT HISTOGRAM
164) 581   FORMAT(F5 1,I4,'  ',60A1)
165)       DO 590 J = 1,JH
166) 590   LINE(J) = BLNK                    /* ZERO THE LINE ARRAY
167) 600   CONTINUE
168) 901   STOP 901
169)       END
170) C
171)       SUBROUTINE LINEAR3(IU,U,C,LCH,NCH)
172) C ******** LINEARIZES 3 DATA CHANNELS OUT OF A TOTAL NCH CHANNELS
173) C         IU = INPUT INTEGER ARRAY   U = OUTPUT REAL ARRAY
174) C          C = COEFFICIENT ARRAY   LCH = STARTING CHANNEL
175)       INTEGER*2 IU(4096)
176)       REAL U(4096),C(4,11)
177)       LCH3 = LCH + 2
178)       DO 100 L = LCH,LCH3
179)       DO 100 I = L,4096,NCH
180)       X = IU(I-1)/409 6
181) 100   U(I) = C(1,L) + X*(C(2,L) + X*(C(3,L) + X*C(4,L)))
182)       RETURN
183)       END
```

Appendix III: Burst Detector

******* THIS PROGRAM COMPUTES THE BURSTING TIMES AND PAGE 0001

```
    1) C ********** THIS PROGRAM COMPUTES THE BURSTING TIMES AND
    2) C                REJECTS THE DECELERATIONS.
    3) C
    4)       PARAMETER (LEN=11)
    5)       REAL A(32),UBAR(LEN),RMS(LEN),OLDT,NOWT,C(4,LEN),UB(5096)
    6)       INTEGER*4 ITOT,ISAVE,KCHN(5)
    7)       INTEGER*2 IU(5096),HIST(40)
    8)       REAL*8 VITAE1,VITASQ,U,U1,AA,BB,V,W
    9)       CHARACTER*32 FNAME
   10)       CHARACTER *5 RUNO
   11)       COMMON /DATA/IU
   12)       DATA HIST/40*0/
   13) C
   14) C    ******* READ IN STORED INFORMATION FORM DISK
   15) C
   16)       PRINT *,'ENTER LAST FIVE CHAR OF RUN NAME : '
   17)       READ(1,'(A5)') RUNO
   18)       OPEN(32,FILE='BURST.DATA'//RUNO,FORM='UNFORMATTED',
   19)      *      STATUS='OLD')
   20)       READ(32) A,C,UBAR,RMS,KCHN,FNAME  /*INPUT STORED INFORMATION
   21)       CLOSE(32)
   22) C
   23) C ******* SELECT THE TRIGGER CHANNEL FOR THE VITA TECHNIQUE
   24) C
   25)       IF(KCHN(4)-1) 5,9,7
   26)  5    CALL TNOUA(' ENTER CHANNEL NUMBER OF FIRST H.F.:   ',38)
   27)       READ(1,*) KCHN(3)
   28)  7    CALL TNOUA(' ENTER CHANNEL # OF H.F. TO ANALYSE:   ',38)
   29)       READ(1,*) ICH
   30)       GO TO 10
   31)  9    ICH = KCHN(3)           /*ICH = CHANNEL # OF H.F.
   32) 10    PRINT *,' CHANNEL #',ICH,' WILL BE ANALYSED.'
   33) C
   34) C ********* SET UP PARAMETERS FOR VITA TECHNIQUE
   35) C
   36)       DT = A(21)              /*DIGITIZING INTERVAL
   37)       U00 = A(22)             /*TOWING SPEED
   38)       NBLK = A(23)            /*TOTAL NUMBER OF [4096]BLOCKS OF DATA
   39)       ISTART = A(24)          /*ISTART = FIRST BLOCK TO ANALYSE
   40)       ISTOP = A(25)           /*ISTOP = LAST BLOCK TO ANALYSE
   41)       NCH = KCHN(1)
   42)       RECL=INT(4096/NCH)*DT
   43)       ICH=ICH-KCHN(2)+1       /*BIAS ICH TO 1ST CHAN INDEX
   44)       AVGU = UBAR(ICH)
   45)       URMS = RMS(ICH)
   46)       PRINT *,'U00 =',U00,'UBAR =',AVGU,'RMS =',URMS
   47)       CALL TNOUA(' ENTER THE VALUE OF UTAU[CM/SEC]:   ',35)
   48)       READ(1,*) UTAU
   49)       DELT = 0.01/UTAU/UTAU
   50)       NSAMP = 10.*DELT/DT
   51)       NSAMP = (NSAMP/2)*2     /*MAKE NSAMP EVEN
   52)       PRINT *,' NSAMP = ',NSAMP
   53)       NS = NSAMP/3*NCH
```

******* THIS PROGRAM COMPUTES THE BURSTING TIMES AND PAGE 0002

```
      FNSMP = 1./NSAMP
      THRES = 1.0            /*TRIGGER LEVEL - 1.2 WAS USED BY RFB AND REK
      ULEV = THRES*URMS**2
      GAM = 0.               /*ZERO INTERMITTENCY
      OLDT = 0.              /*OLDT IS THE FLAG FOR THE LAST DATA POINT
      TRANS = 0.             /*# OF TRANSITIONS(I.E. BURSTS)
      ITOT = 0               /*ITOT COUNTS THE RECORD LENGTH
      VITAE1 = 0.D0            /*VITA SUM FOR MEAN VALUE
      VITASQ = 0.D0            /*VITA SUM FOR MEAN SQUARE VALUE
C
      PRINT *,'BURST STARTING TIME      BURST STOPPING TIME'
C ******** BEGIN THE MAIN LOOP
C
      IBLK = NBLK
      LBLN=(4096/NCH)*NCH+1000
      OPEN(29,FORM='UNFORMATTED',STATUS='OLD',FILE=FNAME)
      DO 210 IB = 1,IBLK
      READ(29,ERR=901)(IU(I),I=1001,5096)
      IF(IB.LT.ISTART) GO TO 210
      IF(IB.GT.ISTOP) GO TO 212
      CALL LINEAR(IU(1001),UB(1001),C,ICH,NCH)
      DO 200 IC = ICH+1000,LBLN,NCH
      ITOT = ITOT + 1                /*INCREMENT POSTITON COUNTER
      U = UB(IC)-AVGU
      U1=U
      VITAE1 = VITAE1 + U           /*SHORT TIME AVERAGE OF U
      VITASQ = VITASQ + U*U        /*SHORT TIME AVERAGE OF U**2
      IF(ITOT.LE.NSAMP) GO TO 200
      JC = IC - NSAMP*NCH
      U = UB(JC)-AVGU
      VITAE1 = VITAE1 - U     /*SUBTRACT OLD DATA POINT
      VITASQ = VITASQ - U*U   /*SUBTRACT OLD DATA POINT
23    VARNCE = VITASQ*FNSMP - (VITAE1*FNSMP)**2   /*COMPUTE VARANCE
      IF(VARNCE + .0001) 100,110,110
100   WRITE(1,101) VARNCE,ITOT,IC,U,VITAE1,U1,VITASQ
101   FORMAT(F10.5,2I8,4F12.5,/)
      XSTOP = XSTOP + 1
      IF(XSTOP.GT.(NSAMP+10.)) STOP 'VARIANCE WAS NEGATIVE'
110   CONTINUE
      IF(VARNCE - ULEV) 150,160,160
C ********* STATEMENT #150 IS FOR I(T) = 0
150   NOWT = 0.
      IF(NOWT - OLDT) 155,190,190
C          STATEMENT 155 IS EXECUTED WHEN EXITING FROM A BURST
155   TRANS = TRANS + 1              /*COUNT THIS LAST BURST
      DUMIB=IB
      DUMIC=IC-1000
      T2=((DUMIB-1.)+((DUMIC-1.)/4096.))*RECL
      WRITE(1,'(2(5X,F8.4))') T1,T2
      ISAVE = 0
      UMIN = 1000.
      UMAX = -1000.
      DO 197 I = JC,IC,NCH
```

```
******* THIS PROGRAM COMPUTES THE BURSTING TIMES AND                    PAGE 0003


  107)        IF(UB(I).LT.UMIN) UMIN = UB(I)
  108)        IF(UB(I).GT.UMAX) UMAX = UB(I)
  109) 157    CONTINUE
  110)        IH = UMAX - UMIN + 1.5
  111)        IF(IH.LT.1) IH = 1
  112)        IF(IH.GT.40) IH = 40
  113)        HIST(IH) = HIST(IH) + 1
  114)        GO TO 190
  115) C ******** IS THIS AN ACCELERATION OR DECELERATION?
  116) 160    IF(UB(IC-NS) - UB(JC+NS)) 150,150,170  /*ELIMINATE DECELERATIONS
  117) C *********** STATEMENT #170 IS FOR I(T) = 1, I.E. INSIDE A BURST
  118) 170    NOWT = 1.
  119)        GAM = GAM + 1.
  120)        IF(NOWT - OLDT) 190,190,180
  121) 180    ISAVE = ITOT                /*SAVE BEGINNING COUNTER OF THIS BURST
  122)        DUMIB=IB
  123)        DUMIC=IC-1000
  124)        T1=((DUMIB-1 )+((DUMIC-1. )/4096. ))*RECL
  125) 190    OLDT = NOWT
  126) 200    CONTINUE
  127) C ********** MOVE REMAINING DATA TO THE BEGINNING OF THE BUFFER
  128)        LSPT = (4096/NCH)*NCH + 1
  129)        JC = 0
  130)        DO 205 IC = LSPT,LSPT+1000
  131)        JC = JC + 1
  132) 205    UB(JC) = UB(IC)
  133) 210    CONTINUE
  134) 212    TREC = (ITOT - NSAMP)*DT        /*TOTAL RECORD LENGTH
  135)        BURSTS = TRANS                   /*NUMBER OF BURSTS
  136)        FREQ = BURSTS/TREC
  137)        FIN = FREQ*DELT
  138)        GAMMA = GAM/ITOT*100.
  139)        WRITE(1,213) THRES,BURSTS,GAMMA,FREQ,FIN
  140) 213    FORMAT(/,' THE BURSTING STATISTICS FOR THRESHOLD =',
  141)       1F4 1,' ARE: ',/,10X,'NUMBER OF BURSTS =',F10.0,
  142)       2/,10X,'INTERMITTENCY FACTOR =',F8.2,' %'
  143)       3/,10X,'FREQUENCY =',F19.2,' HZ',/,10X,'FREQ+ =',F26.5,/)
  144)        CALL HSTER(HIST,40)
  145)        CLOSE(29)
  146)        CALL EXIT
  147) C 901 DATA READ ERR
  148)   901 STOP 901
  149)        END
  150) C
  151)        SUBROUTINE LINEAR(IU,U,C,ICH,NCH)
  152)        INTEGER*2 IU(4096)
  153)        REAL U(4096),C(4,11)
  154)        DO 100 I = ICH,4096,NCH
  155)        X = IU(I)/409.6
  156) 100    U(I) = C(1,ICH)+X*(C(2,ICH)+X*(C(3,ICH)+X*C(4,ICH)))
  157)        RETURN
  158)        END
  159) C
```

```
***** THIS PROGRAM COMPUTES THE BURSTING TIMES AND                    PAGE 0004


      SUBROUTINE HSTER(HIST,N)
      INTEGER*2 HIST(N)
      CHARACTER LINE(40),BLNK,AST
      DATA BLNK/' '/,AST/'*'/
C
C     LOCATE FIRST AND LAST POINT IN HISTOGRAM
C
      IMIN = N
      DO 20 I = 1,N
      IF(HIST(I).LE.0) GO TO 20
      IMIN = I
      GO TO 25
20    CONTINUE
25    IMAX = 0
      DO 30 I = 1,N
      IF(HIST(N+1-I).LE.0) GO TO 30
      IMAX = N + 2 - I
      GO TO 35
30    CONTINUE
35    WRITE(1,39)
39    FORMAT(//,' HISTOGRAM OF THE MAXIMUM VELOCITY AMPLITUDE'
     1,' DIFFERENCE DURING ACCELERATION ',//,' CELL SIZE',
     27X,'# OF',/,2X,'[CM/SEC]',6X,'BURSTS',/)
      DO 100 I = IMIN-1,IMAX+1
      X = I - 1
      Y = X + 1.
      INUM = HIST(I)
      DO 80 J = 1,40
      IF(J.GT.INUM) GO TO 75
      LINE(J) = AST
      GO TO 80
75    LINE(J) = BLNK
80    CONTINUE
100   WRITE(1,101) X,Y,INUM,LINE
101   FORMAT(3X,F3.0,'-',F3.0,I10,2X,':',40A1)
      RETURN
      END
```

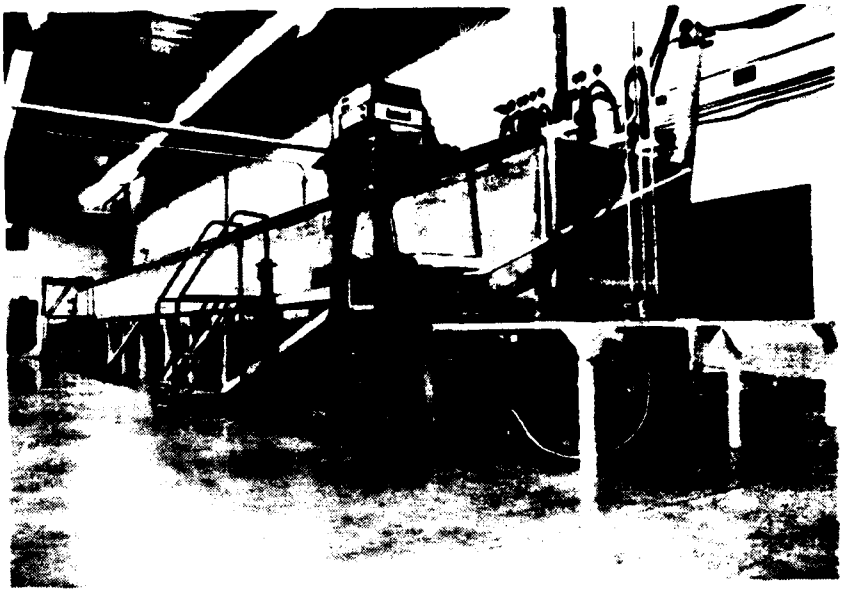

Figure 1. The 18 m Towing Tank

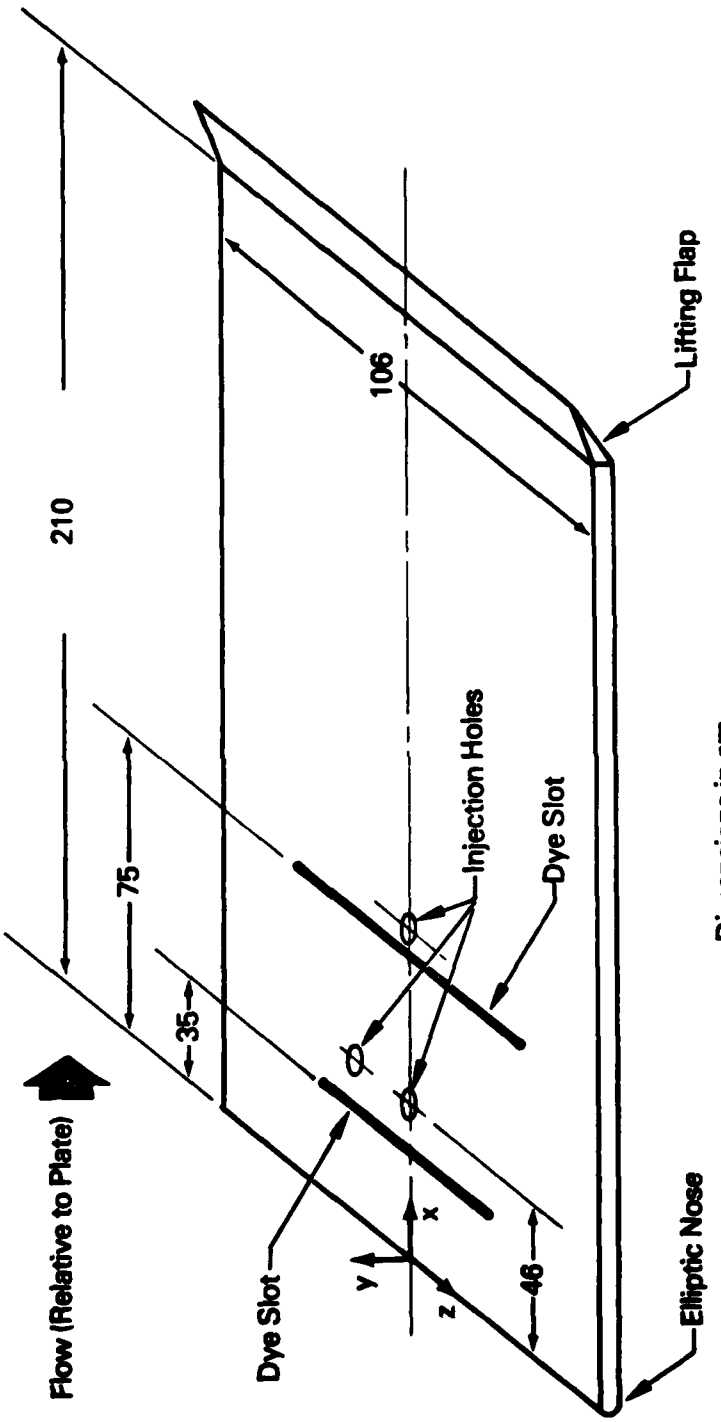

Figure 2. Schematic Diagram of the Flat Plate and Coordinate System

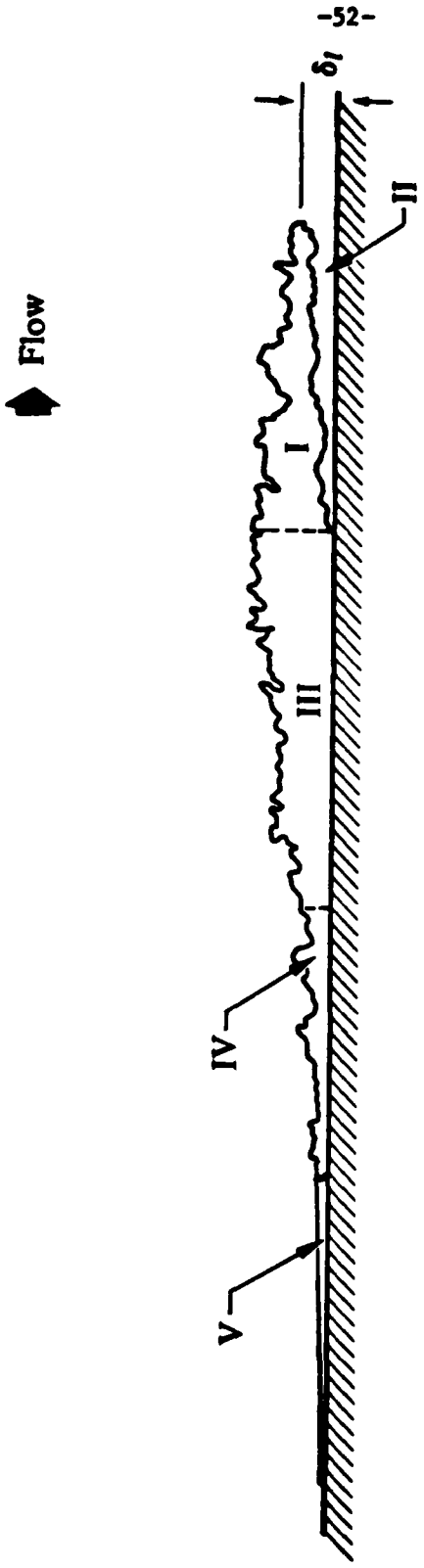

Figure 3. Schematic View of an x-y Cut Through the Turbulent Spot

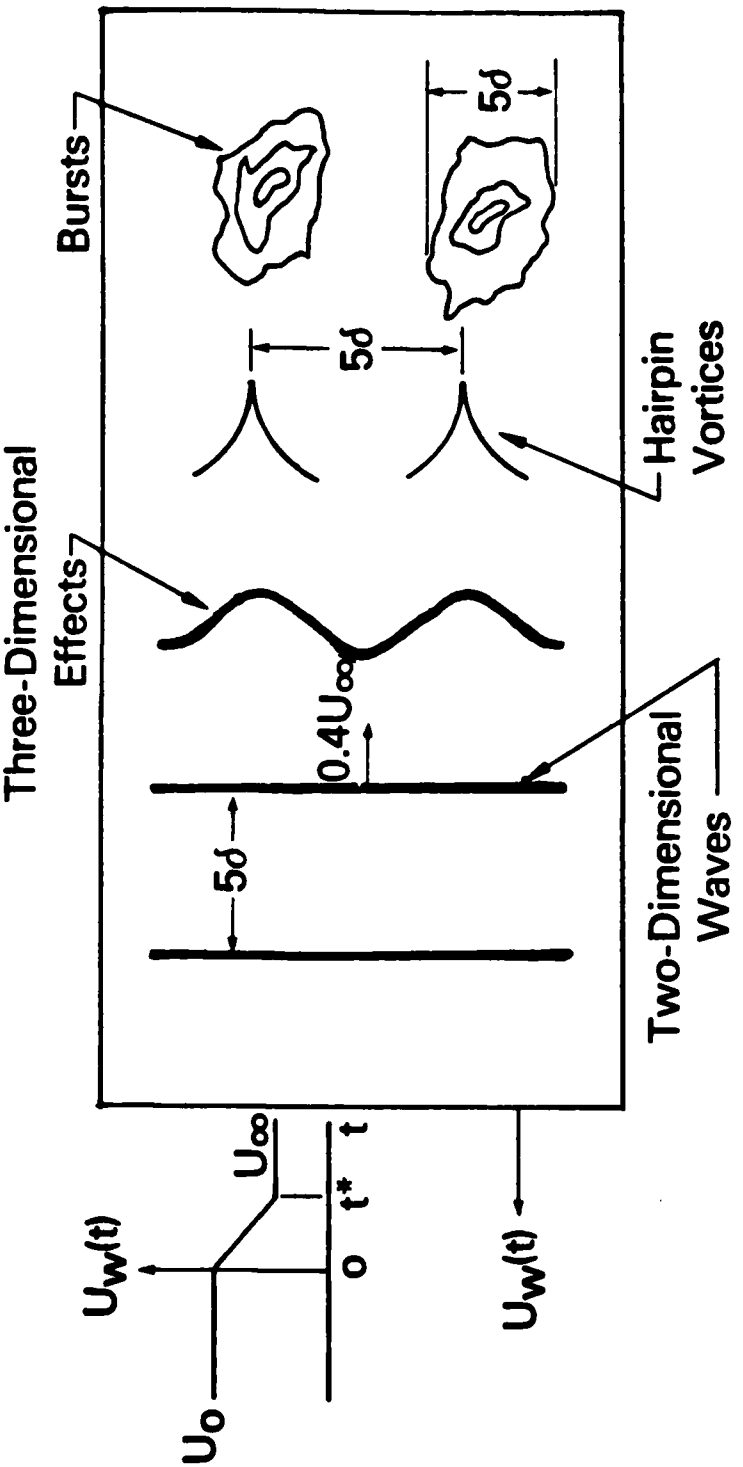

Figure 4. Schematic of Transition Events in a Decelerating Boundary Layer

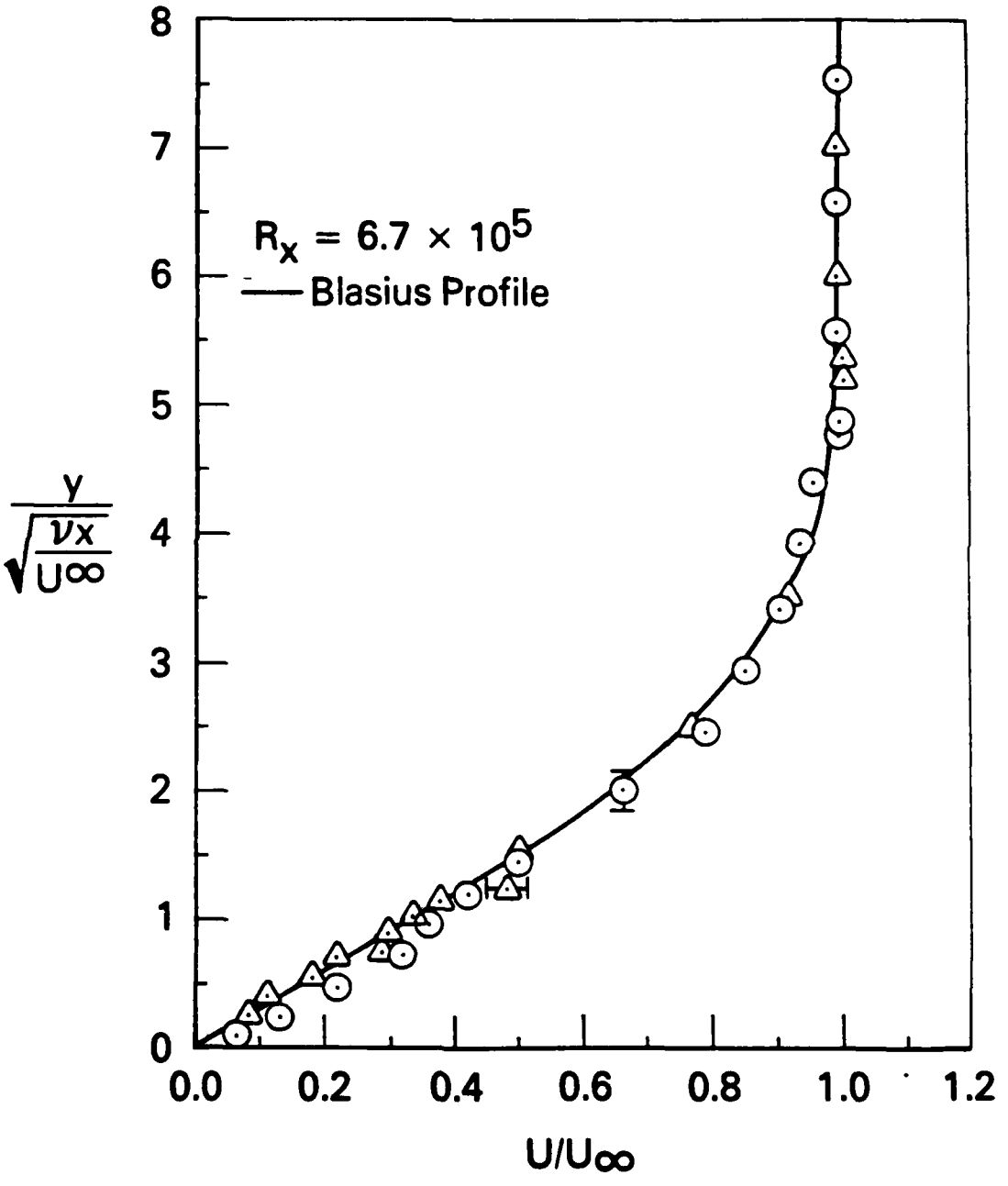

Figure 5. Laminar Boundary Layer Profiles

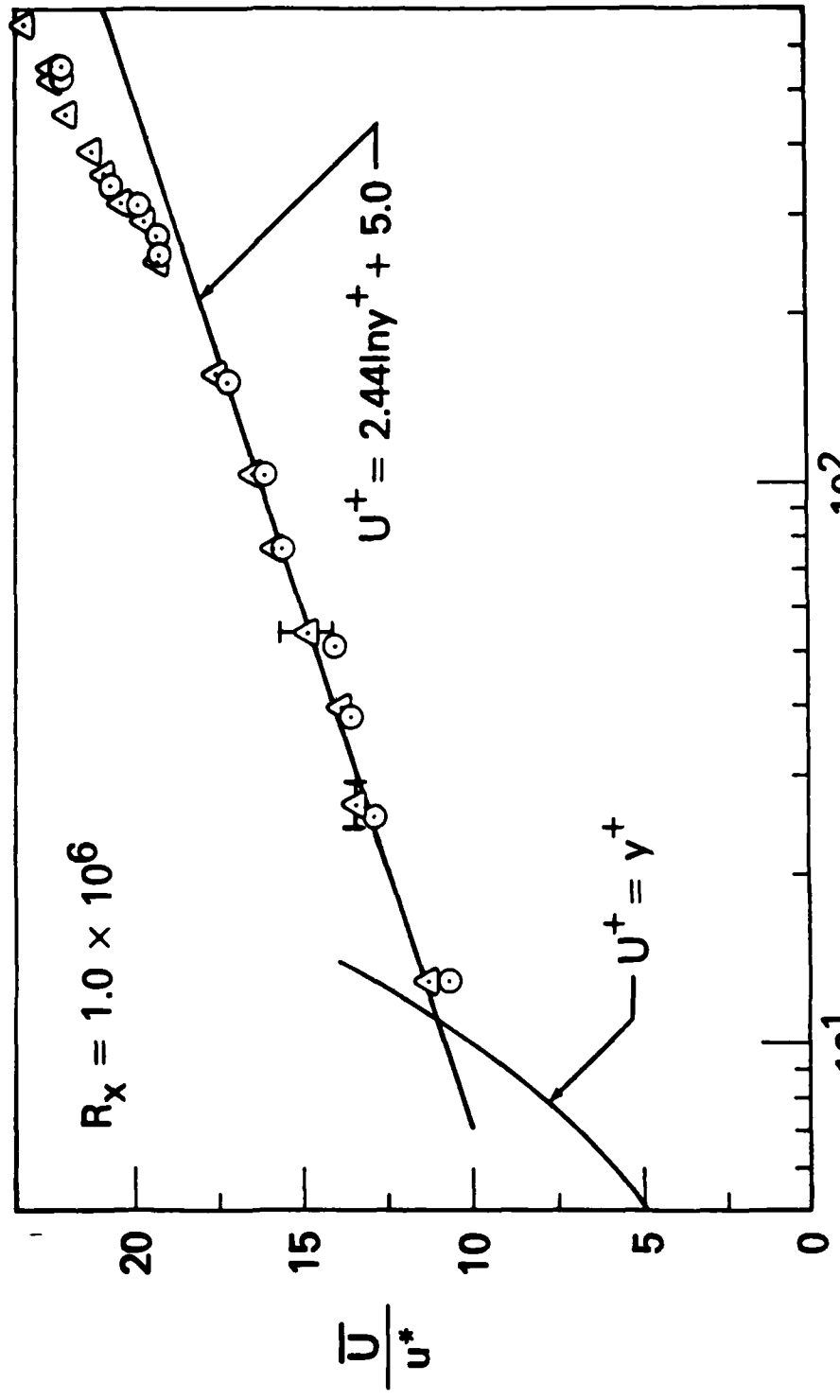

Figure 6. Turbulent Boundary Layer Profiles

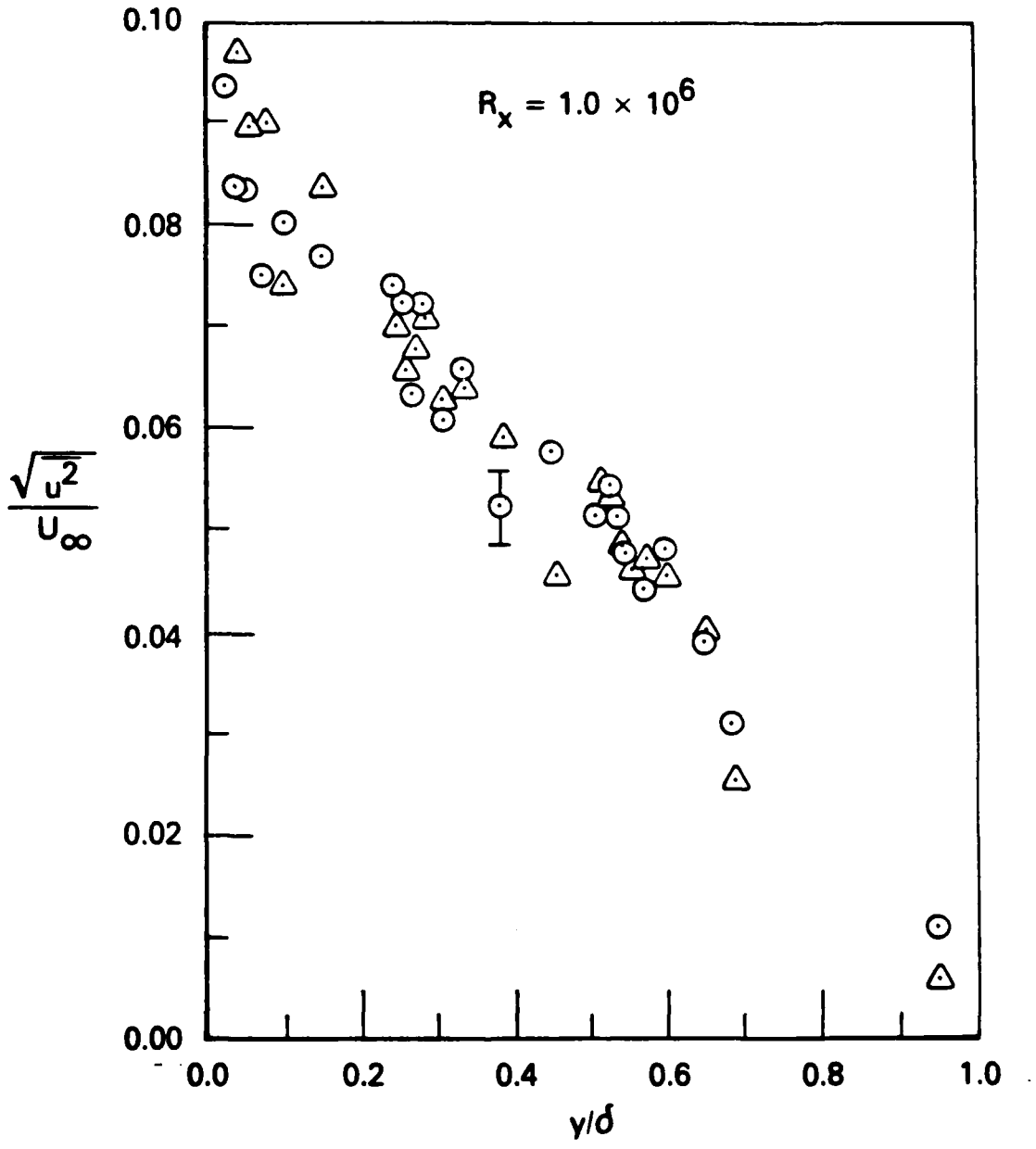

Figure 7. RMS Turbulent Intensity

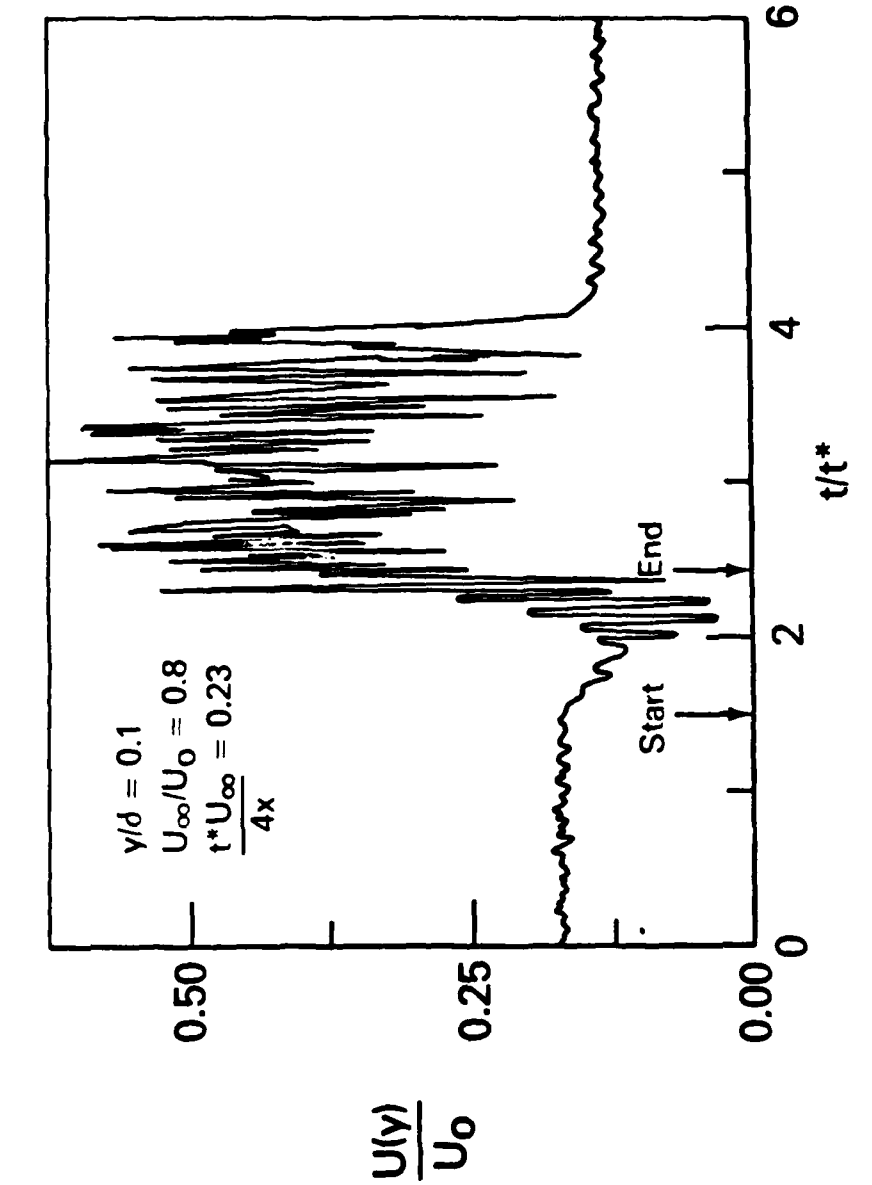

Figure 8. Longitudinal Velocity During Deceleration

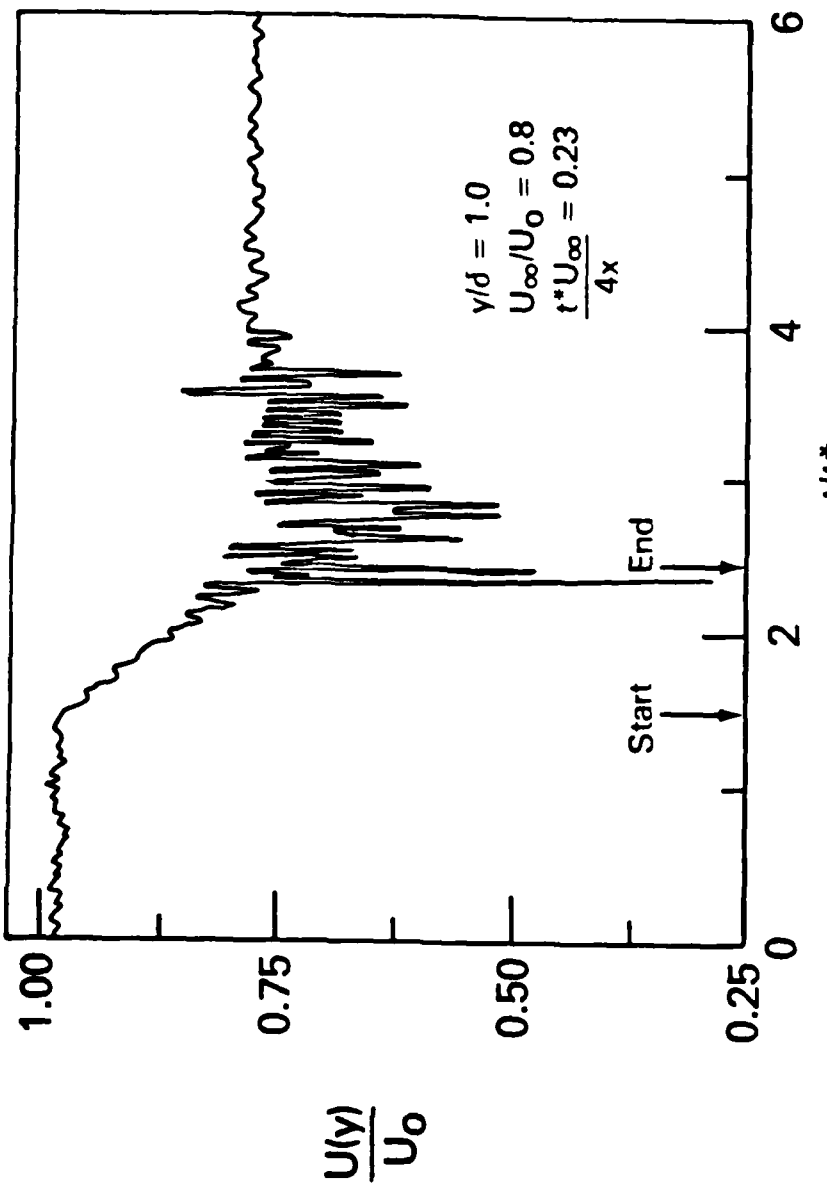

Figure 9. Longitudinal Velocity During Deceleration


FILMED
9-8